Alma Mater Studiorum - Università di Bologna
Cesena Campus

Department of Electrical, Electronic and Information Engineering
“Guglielmo Marconi” - DEI

Second Cycle Degree in Biomedical Engineering
Class: LM-21

THESIS TITLE

Implementation of a Control Algorithm for a Hip Exosuit to Enhance Human Locomotion in Walking and Running

Graduation thesis in

Ageing and Rehabilitation Engineering

Supervisor:
Professor Lorenzo Chiari

Candidate:
Alex Nanni

Co-supervisor:
Professor Luca Palmerini
Professor Lorenzo Masia

Academic Year 2022-2023

Abstract

In the last two decades, the interest towards exoskeletons as devices to help restore a motor functionality and to enhance the human performance has largely grown. Among them, soft exoskeletons, or "exosuits", are becoming popular thanks to their lightweight structure and their potential use in activities of daily living. Exosuits for lower limbs have been created to assist multiple movements with promising results, but only few devices have been designed for running. The main limitation of such devices is the necessity to reverse the motor direction of rotation to alternately support the proper leg, which is not achievable at high human cadences because the motor would work against its own inertia. Therefore, a new design for a hip exosuit for both walking and running assistance is proposed, based on a Cardan Gear mechanism: the rotation of the motor is converted into a linear, alternated motion of an actuator that preserves a limited amount of cable to provide to the user, hence the motor can continuously spin in one direction. A single motor drives both legs (underactuated exosuit) and assists them during hip extension. This preliminary version of the exosuit is intended for off-board testing purposes and relies on basic biomechanic principles, avoiding the use of complex machine learning processes. Three Inertial Measurement Units (IMUs) are used to acquire the relevant gait parameters and to detect the actual locomotion mode in real-time to create the proper reference position command for the motor. Experiments have been conducted to test the ability of the device to follow the user's motion, showing optimal outcomes at every human cadence, and the algorithm for locomotion mode detection reported an overall accuracy higher than 98%. These promising results push us towards the further development of the device, with subject-specific profiles of assistance and with the ultimate purpose to reduce the user's effort in walking and running.

Contents

Introduction

In the relentless pursuit of augmenting human capabilities, the integration of technology into our daily lives has become increasingly prevalent. One area where technological advancements hold significant promise is in the realm of mobility assistance, particularly for activities as fundamental as walking and running. As our understanding of biomechanics and robotics has matured, the development of exoskeletons and exosuits — devices designed to amplify and support human movement — has emerged as a groundbreaking frontier in the field of assistive technologies.

Exoskeletons have been extensively researched and developed to aid the movements of various joints in the body. They can involve a single degree of freedom (DOF), for example, flexion and extension of the elbow or the knee, or multiple DOF, like hand movements.

They can be subdivided into two main classes: medical and non-medical. The first group includes both rehabilitative and assistive devices which are intended to provide guided movements by decreasing the load action on the wearer or physical support for daily living activities. They may be employed in elderly people with atrophied joints who cannot fully perform conventional movements but also in people with motor disabilities caused by illness or accident. It is well known, indeed, that it is possible to improve motor skills through rehabilitation therapy based on passive movements exercises, which involves repetitive movements in the affected joint, leading to a better recovery of the motor skills both in the short and long term. On the other side, non-medical exoskeletons are enhancers for people without any motor disabilities: they are designed to improve the skills of the user and to provide an increased capability of carrying heavy loads with minimal effort, giving a boost to the individual in terms of velocity, power and endurance. They are used for work, military and space purposes, and the typical operators can be soldiers, industry workers or fire fighters in order to provide physical relief to the user [1].

Among all the ideal characteristics that an exoskeleton should have, either related to the final purpose of the device or to the perception and the feeling of the user, portability is probably the one that marks the difference between rigid and soft exoskeletons. Portability is often a direct consequence of the main purpose of the unit: when the intended application is to guide a recovering patient or an impaired person through the rehabilitation process, or when a great accuracy is required, a solid structure is preferred. These functions can be achieved with motor-driven metallic devices, which offer several advantages including the reliability and robustness of the structure and the ability to precisely transmit forces and torques to a body segment. However, due to the weight and complexity of the design, the final structure is heavy, non-portable and usually uncomfortable for the user, and it often requires trained personnel to be installed.

Therefore, in the last 15 years researchers have been working also on soft exoskeletons, or "exosuits", which offer much lighter and portable solutions. Exosuits replace many or all of the big and rigid components with soft, thin and flexible ones, guaranteeing greater comfort to the user. The hard components that cannot be substituted, such as controllers and batteries, are often placed in a backpack or separately to reduce weight. They are easier to install and to transport, allowing them to be used outside the clinic and without any supervision; for these reasons, they gained a lot of interest throughout the years and great efforts are being done in this direction.

This thesis aims to highlight the potentialities of exosuits through the presentation and description of a new and modern system to assist walking and running. This project has roots in the previous works of the ARIES LAB of the University of Heidelberg, led by Prof. Dr. Lorenzo Masia: in the last few years they have been massively dedicating to support and improve the functionalities of the lower limbs and they have created multiple exosuits for various applications, like walking, sit-to-stand assistance, climb and descend stairs and also jogging. All these devices, which rely on different sensors and control strategies, are tendon-driven and have reported very promising results in terms of decreasing the energy expenditure of the user, but failed in providing support during running. These exosuits, indeed, are equipped with one motor or two motors that alternate the direction of rotation according to the intended movement of the legs; however, if the walking frequency is too high, the motor will be no longer able to promptly change direction because of its inertia and the resulting movement will be useless, or even harmful, for the user. Furthermore, the lack of devices for both walking and running assistance is also a matter of detection of the current locomotion mode: this operation can be quite tricky in real-time applications, given the limited amount of sensors that such system can include to guarantee an efficient functioning, but it nevertheless essential because walking and running exhibit clear differences in the gait pattern and they must be investigated separately.

Our project finds place in this domain and tries to address the mentioned limitations. The approach adopted to overcome the limit of motor inertia is to make the motor spinning without reversing the direction of rotation, while preserving a limited amount of cable to supply or withhold to the legs. This is possible using a Cardan Gear mechanism which has a much larger bandwidth in order to withstand the higher human cadence in running conditions.

Such innovative hardware device is supported by a traditional control scheme based on the identification of gait phase, obtained as the angle between two vectors (hip angle and hip angular velocity). This strategy has proven to be reliable and does not necessitate computational load, bringing the advantages of simplicity, adaptability and lower complexity in computational terms, translated in a smaller delay between the creation of the reference command and the actuation. In addition, the purpose of walking and running classification is addressed by developing and testing two algorithms, which rely on completely different biomechanical principles.

This thesis addresses the characteristics of an underactuated hip exosuit, that is a system where a single motor is used to coordinate the assistance to both legs. After a brief overview of the biomechanics of walking and running and a general state-of-the-art about hip rigid and soft exoskeletons, the thesis describes the main hardware features of the system and fully illustrates the control scheme of the new soft underactuated exosuit for walking and running assistance, focusing on the principal differences with the devices specifically designed for walking only. After the creation of the actuation unit, the device is tested off-board to evaluate its ability in promptly following the user's gait in both walking and running conditions and its accuracy in the detection of the current locomotion mode: a fundamental initial step for the development of such modern exosuit.

Chapter 1

Human locomotion and assistive devices

1.1 Biomechanics of walking and running

Walking is an extremely efficient activity: legs, trunk and arms are coordinated to produce the least expensive movement in energetic terms and to maintain stability during gait.

A gait cycle is a periodic cycle between two consecutive occurrences of the same gait event with the same foot [2]. These reference events are usually the initial contacts of the foot with the ground, also called Heel Strike (HS). Typically, a walking gait cycle is divided into two main phases: the stance phase, that accounts for approximately 60% of the entire cycle, starts when the foot strikes the ground (HS) and terminates when it leaves the ground, in the Toe Off (TO) event of the same foot, while the swing phase, approximately 40% of the gait cycle, refers to the time when the foot is not in contact with the ground and goes from the TO to the HS of the same foot. Since the swing phase is characterized by a single limb on the ground, this is also called single limb support, whereas double limb support refers to when both feet are on the ground. A walking gait cycle exhibits two double support phases and two single support phases. Figure 1.1

Conversely, a running cycle consists of two phases of single support and two phases of "double float", when there is no contact with the ground. For each leg, the stance is the first single support phase of the corresponding cycle and is about 40% of the entire gait cycle, while the swing accounts for approximately the 30%. Figure 1.2

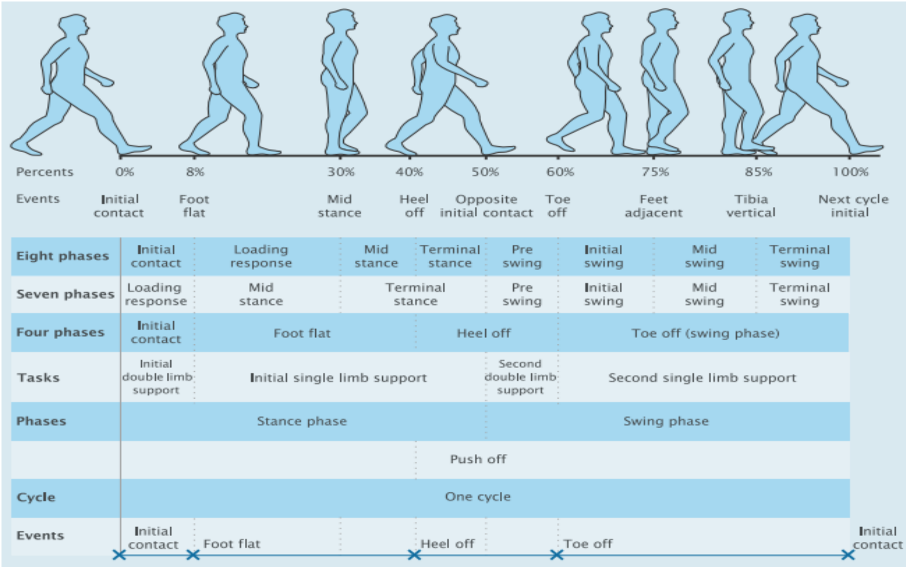

Figure 1.1: Gait phases in Walking

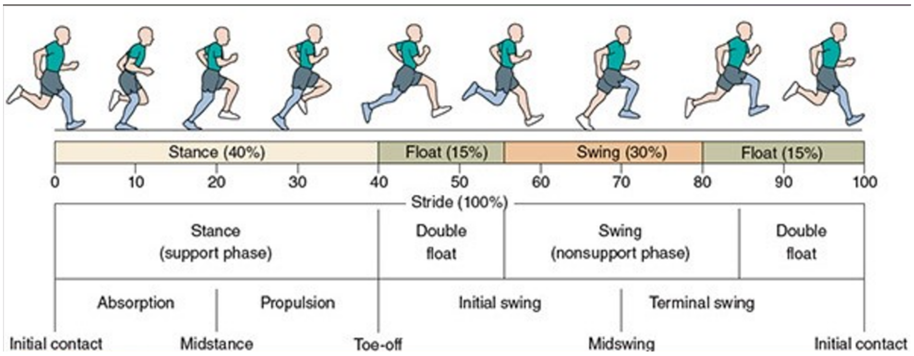

Figure 1.2: Gait phases in Running

1.1.1 Energy-related differences

The distinct difference between walking and running gaits is in the ground reaction force (GRF) patterns. In human walking, there is always at least one foot in contact with the ground, while running is a series of bouncing impacts with the ground; this means that running presents a substantially higher magnitude vertical component of the GRF than walking [3]

This difference is in the spotlight when investigating the propulsive phase in the running gait pattern. This portion of the gait cycle occurs in the second half of the stance, from “mid-stance”, the point at which the standing foot passes beneath the hips, to toe off. The propulsive moment is fundamental to create an efficient gait profile: the task is to generate a strong propulsive drive to push onto the next stride, and the propulsion is effectively created by pushing the ground away, behind the forward centre of mass. Elite runners have the ability to extend powerfully through a large range of hip extension motion before the foot leaves the ground producing a huge stride length. The potential energy stored in their hip flexor muscles and tendons during this powerful hip extension enables the massive elastic recoil in the recovery phase. The propulsive phase is a key to develop running speed and efficiency; therefore, assisting hip extension is more convenient.

Another consequence of the different vertical component of the GRF between walking and running is found in the completely dissimilar patterns of mechanical fluctuations of the center of mass (COM) across the gait cycle. During walking, the body vaults over a relatively stiff stance limb and the COM reaches the highest point at the middle of the stance phase, where the gravitational potential energy of the COM is maximized. This does not happen in running: the stance limb is compliant so that the joints undergo flexion in the first half on the stance and extension in the second half, causing the vertical displacement and gravitational potential energy of the COM to reach their minimum values at mid-stance. On the other side, the kinetic energy profile is similar for walking and running and the minimum value is obtained at mid stance. Since the COM profile is a sinusoidal wave with the same period of the gait cycle, the COM position at HS is exactly the opposite of what happens at the mid-stance: the COM reaches the lowest point during walking and the highest during running.

As a consequence, in walking the gravitational potential energy and the kinetic energy are about 180° out of phase: before mid-stance the COM gains potential energy and loses kinetic energy, after mid-stance the opposite behavior is detectable. Because the fluctuations of the two forms of energy are similar in magnitude and they are half-cycle out of phase with each other, substantial pendulum-like exchange occurs between the two forms of energy, and the energy transfer mechanism in walking is often referred to as “inverted pendulum”. About 60-70% of mechanical energy required to lift and accelerate the COM is conserved by this energy transfer mechanism, which is maximally efficient at moderate walking speed and more ineffective at very low and very high walking speeds. In contrast, these fluctuations are nearly in phase with each other in running and such energy transfers are very limited, conserving less than 5% of the mechanical work required to move the COM. Because the movements of the COM are similar to a bouncing ball, running is often referred to as "bouncing gait" and modeled as a simple spring-mass model represented by a single linear "leg spring" and a point equivalent to the body mass. Figure 1.3

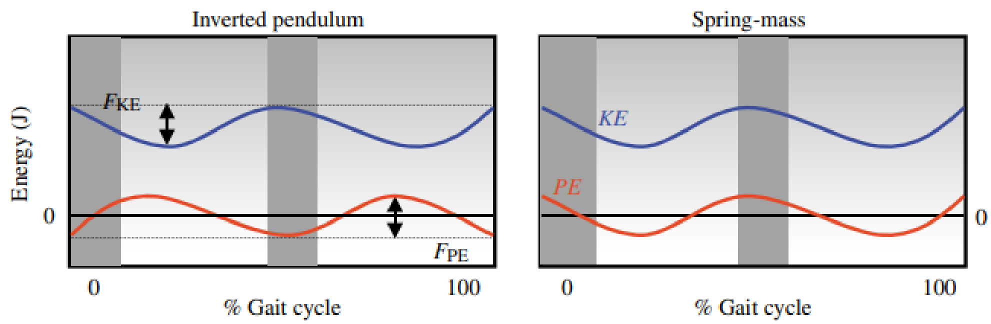

Figure 1.3: Energy profile of walking (left) and running (right)

1.1.2 Transition between locomotion modes

The shift from walking to running is not a smooth and continuous event and it is characterized by sudden changes in GRF, ground contact time and movements of the COM. The walk-run transition usually arises when running requires less metabolic energy than walking, and the speed at which this occurs, according to the inverted pendulum mechanics, can be estimated by taking into account gravity. The gravitational force on the COM must be at least equal to the centripetal force needed to keep the COM moving in a circular arc as it vaults over the stance limb. The ratio between the centripetal force and gravitational force is defined as Froude Number and it is predicted that humans usually adopt a walking gait only at speeds where the Froude Number is less or equal than 1 [3].

$$Froude\ Number = \frac{centripetal\ force}{gravitational\ force} = \frac{mv^2/L}{mg} = \frac{v^2}{gL}$$

1.2 Hip - Anatomy and Function

The hip is a spheroidal, or ball-and-socket-type, synovial joint stabilized by bony and ligamentous restraints. It is formed by the articulation of the femoral head with the acetabulum and connects the axial skeleton with the lower extremity (Figure 1.4.A). It acts as a multi-axial joint upon which the upper body is balanced during stance and gait. The balance and stability provided by the hip joint allow motion while supporting forces encountered during daily activities: the congruity of the femoral head with the acetabulum allows the rotational motion required to perform these tasks without any detectable translational motion which would destabilize the joint and increase the risk of dislocation. [4]

Hip is a joint with 3 degrees of freedom and performs flexion/extension movements in the sagittal plane, abduction/adduction in the frontal plane, rotation in the transverse plane. The hip joint's ability to balance forces through its full range of motion provides the stability required to execute everyday tasks such as standing upright, maintaining a smooth and balanced gait, rising from a chair, and lifting weight from a squatting position. The inherent stability provided by the osseous anatomy of the joint coupled with the stabilizing forces of the fibrous capsule and neuromuscular anatomy defines the absolute limits of motion of the hip joint before the occurrence of bony impingement.

- Flexion – 120 degrees
- Extension – 10 degrees
- Abduction – 45 degrees
- Adduction – 25 degrees
- Internal Rotation – 15 degrees
- External rotation – 35 degrees

Smooth gait is achieved through a series of concentric and eccentric muscular contractions, both voluntary and involuntary. A complex neuromuscular loop receiving proprioceptive feedback from both the position of the body and intrinsic muscular properties, such as muscle spindle fiber and sarcomere length, maintains the proper position of the femoral head within the acetabulum.

Compared with the human ankle joint, the hip joint needs higher metabolic cost for the creation of similar mechanical joint power owing to the differences in the muscle characteristics. Hence, hip joint devices are also a promising strategy because high positive torque is provided by the hip during the activities of daily living [5].

There are two main issues in gait: one is the forward stride length, which is regulated by hip extension/flexion, and the other is stride width, which is crucial for stability and is controlled by hip abduction/adduction. However, most of the supportive devices, especially those regarding the hip, are created to assist the forward gait pattern rather than the medio-lateral stability (Figure 1.4.B). [6]. In the sagittal plane, among others, the *psoas major* and *gluteus maximus* are responsible for respectively flexion and extension. (Figure 1.4.C and D).

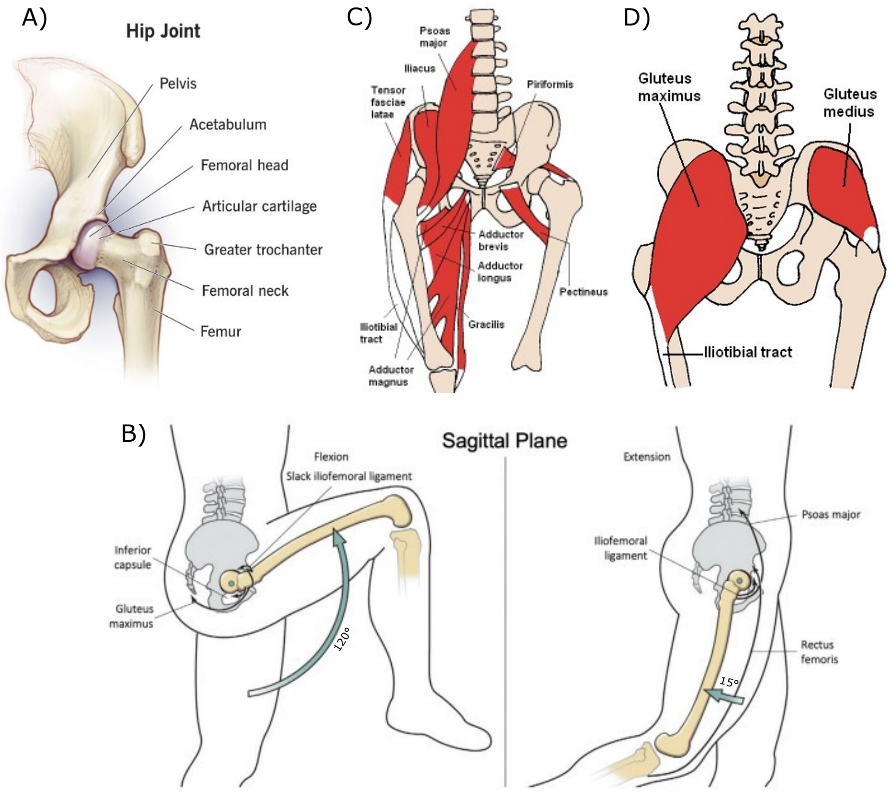

Figure 1.4: **A**. Principal bones of the hip. **B**. Hip motion in the sagittal plane. **C,D**. Anterior and posterior view of hip muscles [7]

1.3 Hip Devices: State-Of-The-Art

Exoskeletons for lower limb assistance began to appear more than 70 years ago, when in 1948 Professor Bernstein in the former Soviet Union designed the first motor-driven lower limb exoskeleton system. Then, Professor Vukobratovic from Yugoslavia developed the first cylinder-driven lower extremity exoskeleton for patients with spinal injuries in 1971 [8]. The improvement of these devices was relatively slow until the end of the 20th century, when the introduction of new components such as sensors and high-performance processors enabled a much faster evolution of such technological systems. These devices were first employed in military research, but in the past 20 years researchers started to address their work for health and rehabilitation purposes with the attempt to progressively make exoskeletons accessible and useful for people, a process that is still going on today [9].

A fundamental milestone in this progress occurred in 2013 when Malcom et al. [10], developing a tethered active ankle exoskeleton, were the first to break the metabolic cost barrier, considered as the gold-standard method for assessing lower-limb exoskeleton performance because it is an objective and easily attainable measure of effort. In particular, they managed to improve their participants' walking economy (to reduce their metabolic cost) during walking by 6%. From that moment onwards, several systems were designed with the goal to reduce the wearers' effort while travelling; most of them are intended for walking, but running has a growing appeal due to the desire of addressing each modality of the human locomotion [11].

Among all exoskeletons, robotic hip devices combine the robot power and human intelligence, and they can furnish controllable assistive force/torque at the wearer's hip joints with an anthropomorphic structure. One application of hip exoskeletons is gait rehabilitation: they can train the wearers' muscles and coordinate their movements for therapeutic exercise. They release therapists from the heavy burden of rehabilitation sessions and provide long training programs for the patients with good consistency. In alternative, since human effort is related to the metabolic expenditure, the other application of this kind of exoskeletons is to enhance human performance such as augmenting the human strength and endurance. The interest towards hip exoskeletons not only for rehabilitation applications but also for the purposes of human performance augmentation began after researches demonstrated that the hip joint plays a fundamental role in the provision of mechanical power during a gait cycle, up to 45% [5].

1.3.1 Hip exoskeletons

A robotic hip exoskeleton was developed to increase the mobility of the wearers' hip joints and reduce their metabolic cost during walking by van Wijdeven [12]. The exoskeleton is composed of the waist part, two thigh parts, and two leaf springs, with four DOFs in total. The leaf springs are designed to be parallel to the human leg to capture the negative work that an individual does during a gait cycle. The exoskeleton has a weight of 4.15 kg. Treadmill gait trials with a healthy individual were conducted and The testing results validated the effectiveness of the exoskeleton in reducing the energetic cost of human walking.

Kang et al [13] developed a robotic hip exoskeleton to reduce the metabolic cost of healthy individuals during walking. The exoskeleton weighs about 7 kg and is actuated by two series elastic actuators (SEAs). The SEA, which is able to provide a peak torque of 60 Nm, is composed of an electric motor, a timing belt transmission, a ball screw transmission, and a fiberglass leaf spring. Experiments were conducted in ten able-bodied individuals and the results demonstrated a U-shaped trend between the exoskeleton assistance and the wearer's metabolic cost.

Miller-Jackson et Al [14] created a robotic exoskeleton to assist hip flexion that exploits pneumatic rotary actuators (PRAs) to transmit torques in the direction of the hip flexion. They structure comprises tubular jammed beams (TJBs) - soft beams with variable stiffness that enable the device to fit each user's body shape - an array of PRAs and strategic ergonomic attachments. Their actuation system is successfully able to provide the target torque output at a specific target position, achieved at a pressure of approximately 86 kPa. Furthermore, the test conducted on ten healthy subjects while performing leg raise and walk at different speeds reported a lower effort in terms of muscular activation with respect to the condition without exoskeleton.

A device for the assistance of both walking and running has been implemented by Zhou et Al [15]. They proposed a hip unpowered exoskeleton to regulate metabolic energy of the hip flexion during the common energy consumption period. It uses exo-tendons acting in front of the hip joint to recycle the negative mechanical energy which is subsequently released to assist hip flexors. The design is pretty similar to that of an exosuit: the lightweight structure is closed to the human trunk minimizing the metabolic penalty introduced by the mass of the device, it consists of a waist frame, a waist belt, but still presents rigid force leverages and thigh braces and connected rods. After testing the exosuit for the evaluation of the optimal spring stiffness for the unit, the experiments on nine healthy male subjects reported a consistent metabolic reduction and a generally reduced activation the *rectus femoris* across the different testing condition, while the other muscular activities showed no significant changes.

1.3.2 Hip exosuits

As a walking assistive device, adding the device's mass to the wearer's body is inevitable, resulting in augmented energy expenditure of the user. It is reported that adding 4 kg of mass to the waist does not significantly increase energy expenditure, while adding 4 kg of mass to the thigh, foot or shank consumes more energy compared with the waist. [16] Thus, the weight of a device should be as low as possible, and the amount of the weight should be distributed to the waist as much as possible.

The introduction of exosuits avoids problems of needing to align a rigid frame precisely with the biological joints and their inertia can be extremely low. These two elements virtually eliminate resistance to motion, thus permitting close to natural kinematics. Moreover, systems should also be designed in order not to limit the hip motion in the ab/adduction direction or in rotation around the leg axis, in particular for use in daily activities

1.3.2.1 Walking

Asbeck et Al [17] developed a powered exosuit to assist hip extension during walking. Their design includes a backpack frame and uses geared motors to retract webbing ribbon connected to a thigh brace on each leg. The webbing allows to measure the force inside the actuation unit, leading to a more compact and robust unit with no wiring or sensors outside the unit. The system also includes two footswitches to estimate the user's gait phase and cadence. The system has been tested on a single wearer and was proven to be useful in providing the correct assistance during hip extension between 90% and 15% of gait cycle time, contributing up to 30% of the nominal biological moment for walking. However, beside the very small number of subjects, a limitation is that the actuation unit assumes that the person maintains a constant velocity across different strides to estimate the following gait cycle events and to determine the specific motor pull's line up.

Jin et al. [18] proposed a new soft robotic suit for energy-efficient walking in activities of daily living for elderly people. Since the latter generate less ankle plantar-flexor power but more hip flexor power compared with young people, the exosuit is designed to assist hip flexion to reduce the burden of the hip joint. The core of the unit is a winding belt which is elastic to absorb undesirable reaction forces in case of significant control errors or disturbances, thus guaranteeing safety. The whole system, with a weight of 2.7 kg, was tested on nine healthy elderly subjects during self-selected speed walking and the results showed that, when the exosuit is powered on, it provides significant reduction of the energy consumption of the subject and an improvement in kinematic gait features of the subjects compared to the condition of exosuit powered off, but still worn.

Kim et al. [19] explored the potentiality of the human-in-the-loop optimization to identify an individualized profile of assistance. This technique consists in the real-time estimation of a physiological parameter (metabolic cost in this case) which allows to continuously modulate the amplitude and the timing of the peak force applied to the joint, and serves to tackle high inter-participant variability in response to any given assistance. The experiments showed a consistent reduction in the net metabolic cost and to a very low peak torque magnitude compared to analogue devices.

Tricomi et al. [20] built an underactuated hip exosuit to assist hip flexion during walking. Their device has an overall weight of 2.2 kg, it can provide up to 12 Nm peak torque for each leg and it has an autonomy of 10 h of continuous operation. Their motor command derives from the estimation of the gait phase, which starts from the tracking of the hip flexion angle and it is performed by Adaptive Oscillators, a matematical tool able to synchronize with a rhythmic and periodic signal by continuously estimating its fundamental features. This approach allowed them to simplify the sensory apparatus of their exosuit, solely based on IMUs, with the purpose to address simplicity and lightweight requirements. They tested the their device on 6 healthy subjects during slow walking activity, reporting a reduction in the muscular activity of the relevant muscles and confirming a symmetrical assistance between legs.

Cao et al. [21] designed a new exosuit working in three assistance modalities: flexion, extension or flexion/extension. The actuation system includes two independent units for flexion and extension and four Bowden cables to transmit the assistive force to the thigh brace; furthermore, two load cells, an Inertial

Measurement Unit (IMU) and a pressure insole module are placed on each leg, for a total weight of about 4 kg. The trials were conducted on three healthy subject while carrying an additional load of 15 kg or with only the exoskeleton on. In both conditions, the assistance provided by the exoskeleton in each of the three modalities is significantly better than the no exoskeleton mode, while the flexion/extension approach is more effective than extension only, which is better than flexion only.

1.3.2.2 Running

In running, more than in walking, the body's center of gravity is shifted up and down, therefore it is more crucial to wear the soft exosuit in the form of a belt on the waist compared to wearing it on the rest of the body.

Chen et al. [22] realized a powered exosuit to assist hip flexion during running. Their device has a mass of 1.932 kg and consists of two high-power low-inertia motors, control unit, load cells, Bowden cables and IMUs communicating via Bluetooth. After collecting the biological hip moment of multiple subjects, they were able to provide a real-time adaptive assistance based on the previous gait cycles. Analysis at three different speeds showed that the metabolic cost is higher as the running velocity increases and that the exosuit decreases the subject's effort compared to no exosuit at all or in case of disabled assistance.

The design of Yang et al. [23] is extremely light-weight (only 0.609 kg) and adjustable for any body shape. Elastic bands are employed: they elongate during extension phase and deliver energy to support the leg during hip flexion. Since the optimal profile of assistance varies among individuals, they tested three different levels of stiffness and obtained a U-shape trend in terms of metabolic rate from no assistance at all to the maximum stiffness, indicating that a higher stiffness does not always correlate with a greater assistive force because it also affects the kinematics of the movement, resulting less effective than a low or medium level of assistance. Furthermore, they set a generally valid angle at which the hip torque changes from extension to flexion, but not all subjects may satisfy this assumption, and in that situation they will require additional biological extension movements which will increase the metabolic burden.

Finally, Nasiri et al. [24] developed an unpowered exosuit of 1.8 kg with a torsional spring as main feature. This component allows to apply a hip torque with is linearly proportional to the hip joint angle. The experiments conducted on non-professional aerobic athletes confirmed a reduction of the metabolic cost wearing the exoskeleton. They also tried to adapt this system to assist human walking; however, it resulted to be ineffective because in walking, unlike running, during the swing phase (especially from 50% to 70% of the gait cycle) the hip muscles are silent and the presence of a linear spring disrupt the performance and prevents having a passive swing, leading to a greater effort from the user.

1.3.2.3 Walking and Running

The exosuit realized by Kim et al. [25] is currently the only device which can efficiently give support to both walking and running. The design presents the control and actuation unit placed in the wearer's back, including a single motor, an incremental encoder, a servomotor driver and a replaceable battery, whereas two load cells and two IMUs are attached to the thigh wraps. The timing of maximum hip flexion is detected by the IMUs and allows the controller to deliver a consistent hip extension force profile during the gait cycle which is adjusted, step by step, using a force-based position controller. Tests conducted on nine healthy subjects during level treadmill activity reported that the metabolic rate significantly decreased in both locomotion modes, even though the reduction was more modest compared to that of exosuits specifically designed for either walking or running only. However, the unique feature of this exosuit is the capability to switch automatically from walking to running (or vice-versa) assistive profile thanks to the real-time detection of the locomotion mode. Indeed, the system includes a third IMU on the abdomen to measure the vertical acceleration of the trunk, which is a good estimation of the vertical acceleration of the center of mass (COM) of the person and shows totally different trends from walking to running. Treadmill experiments at varying speeds and slopes showed that the algorithm was 100% accurate in the discrimination, and the accuracy was still almost perfect (99.98%) in the locomotion mode detection during overground experiments on a paved outdoor course with gradual change in speeds, demonstrating the robustness of the algorithm.

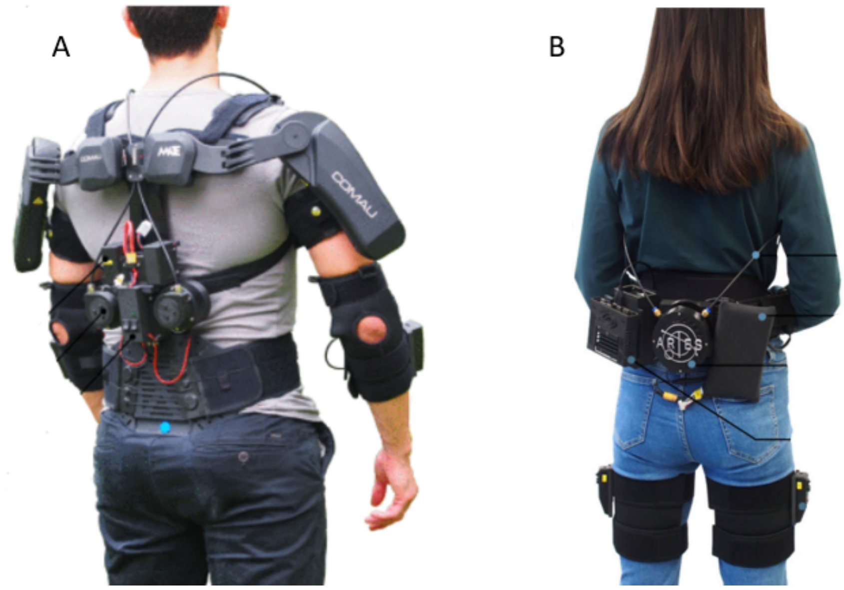

Figure 1.5: Examples of Exoskeletons. **A**) Occupational upper limb exoskeleton [26]. **B**) Soft hip exosuit [27].

Chapter 2

Underactuated exosuit for walking and running

The development of an exosuit to assist both walking and running efficiently represents a step further: not only is there interest in activities of daily living but also in more complex movements which require more performant and tailored equipment. The focus of the project is put on the enhancement of the human performance and the reduction of the user's effort, which are accomplished by assisting the forward gait pattern (and primarily hip flexion or extension) rather than the medio-lateral stability. Therefore, only the hip motion in the sagittal plane is targeted. Moreover, stated the importance of an efficient propulsive phase in the running gait pattern and the relatively lower relevance of flexion or extension assistance while walking, the device has been created to assist hip extension.

The design of the exosuit follows the guidelines of the previous devices of Aries Lab: the system is a powered exosuit with a lightweight structure, the battery must have a sufficient autonomy to run the device for almost the entire day, resistant cable-tendons are used to provide assistance and the control scheme is based on simple biomechanical principles, without adopting machine learning tools. Many characteristics of the new exosuit are inspired from the previous ones [20] [27] [28], but new and peculiar features have been introduced to specifically assess the properties of the running activity, both in the hardware and software design.

2.1 Hardware

The hardware design relies on a hypocycloid actuation approach. A hypocycloid is based on the Tusi Couple, also known as a Cardan Gear mechanism, that consists of two circles, where the smaller one is exactly half the diameter of the bigger one. The small circle rotates at the exactly reversed angular velocity around its centre axis as that centre axis rotates around the centre of the big circle. The scheme is presented in Figure 2.1. In a traditional Cardan Gear approach p = m and the end point of the red dotted line follows a linear trajectory, allowing for the conversion of continuous rotatory motion to alternating linear motion. In this case, however, p > m, hence the resulting trajectory is no longer a straight line but an ellipse. Given this configuration, an additional linear guide is then needed to make the resulting output a straight line, which is represented by the back and forth movement of the cable.

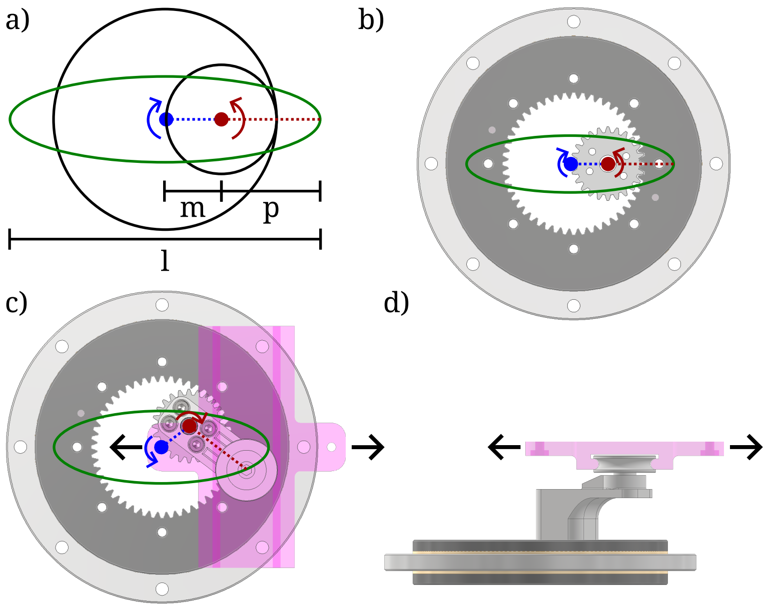

Figure 2.1: Tusi couple in a) as the basis of the mechanical design. Distance of circle centres is m and p the distance from the small circle centre to the endpoint of the red line. b) shows the bigger inner gear representing the big circle and the smaller spur gear representing the smaller circle. The green line represents the ellipsoidal trajectory of the red line endpoint. l is distance between trajectory extremes. c) top view and d) side view of linear guide (purple) to convert ellipsoid trajectory into linear trajectory (black arrows).

The distance between the trajectory extremes is the travelled distance l. The fact that p is longer than m brings the benefit of being able to adjust the travel length of the output by varying the initial angle γ of the red dotted line, therefore enabling control over the amount of cable that is retrieved. The maximum travel, determined by Equation 2.1, is achieved by keeping the angle at 0° as it is in Figure 2.1.a) and progressively decreases to a minimum which corresponds to a rotation of the red line around the red dot by 180° and defined by Equation 2.2. In the present system, the dimensions are m = 12 mm and p = 25.5 mm, therefore the maximum travel distance is l_{max} = 75 mm.

$$l_{max} = 2 \cdot (m + p). \tag{2.1}$$

$$l_{min} = 2 \cdot |m - p|. \tag{2.2}$$

The relationship between the motor angle (or motor position) α to the linear output position x is given by:

$$x = cos(\alpha) \cdot m + cos(\gamma - \alpha) \cdot p \tag{2.3}$$

This position is acquired via a linear encoder (RLM, RLS, Komenda, Slovenia).

Another feature of the mechanism is that one full rotation of the motor exactly corresponds to one complete cycle of the linear guide motion. This means that the alternation frequency of the linear output is directly related to the angular velocity of the motor, and the achievable step frequency of the mechanism is a consequence of the maximum speed of the motor.

The actuation system consists of a T-Motor AK80-6 (24 V, 6:1 Planetary gear-head Reduction Cube Mars actuator, TMOTOR, Nanchang, Jiangxi, China) as main central motor that drives the motion and a Maxon drive system, (made up of a 70 W EC-i 40 brushless motor and a GP 32 C 51:1 planetary gear-head, Maxon, Switzerland) called hereon "secondary motor". The Maxon drive system is only used to adjust the inital angle γ via a worm gear mechanism. Furthermore, a pulley has been added to the linear output in order to double the cable travel, providing a maximum cable travel of 150 mm. An external rotary encoder (AS5047P, AMS, Premstätten, Austria) detects the current position of the motor. It is placed on an external gear that rotates simultaneously to the main motor and whose motion is detected by the rotary encoder. The additional gear is connected to the main one through a timing belt and they have the same diameter, so their revolutions are in the ratio 1:1.

The control system runs on Arduino Mega 2560 (Arduino MRK Wi-Fi 1010, Arduino, Ivrea, Italy) that drives the motor at 1000 Hz via CAN communication. Three IMUs (BNO055, Bosch Sensortec, Reutlingen, Germany) are adopted: two on the lateral side of the thighs (one for each leg), to acquire the meaningful features of the hip gait pattern, and one on the back in correspondence to L5, for the detection of the current locomotion mode. The IMUs stream the data to the microcontroller via a Bluetooth Low Energy module (BLE, Feather nRF52 Bluefruit, Adafruit), whereas the linear and rotary encoders communicate using the I2C protocol. All sensors have a sampling frequency equal to 100 Hz. Figure 2.2

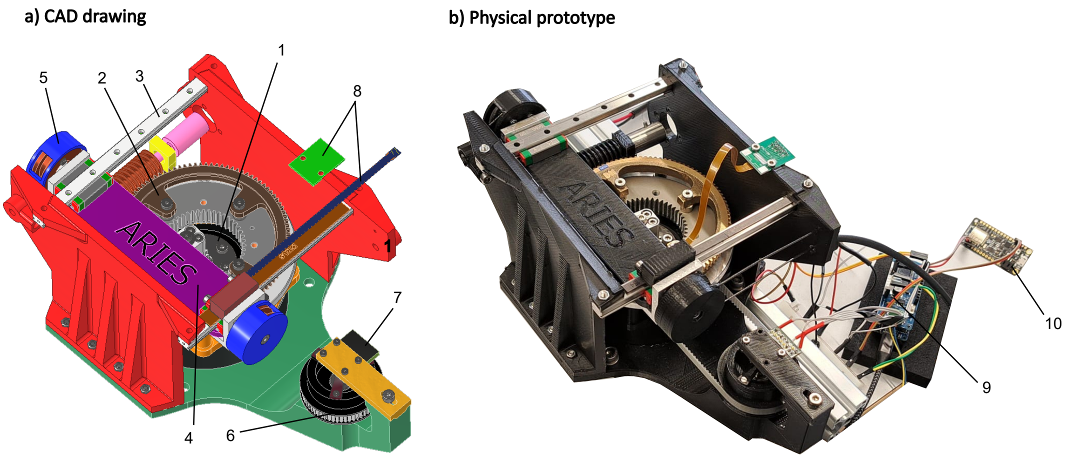

Figure 2.2: a) CAD drawing and b) Physical prototype of the device. The labels refer to: 1) Cardan Gear mechanism; 2) Worm gear mechanism; 3) Slider for linear motion; 4) Linear guide; 5) Pulley for cable; 6) External gear; 7) Rotary Encoder; 8) Linear Encoder; 9) Arduino MKR Wifi 1010; 10) Feather for Bluetooth communication

The actuation system is separated from the suit, with the intention to test an off-board mechanism before creating the final version of the system. The user wears a rigid but comfortable belt with two intermediate anchor points on the back, in correspondence to the conjunction between each leg and the trunk in order to replace the role of the hip joint during extension of the articulation. The cables start from the two extremities of the linear guide, slide through the belt anchor points and are fixed to the posterior portion of the thighs thanks to two thigh wraps, positioned at approximately half of the length of the thigh segment. The belt and the medio-lateral position of the intermediate anchor points are both adjustable to fit any body size and to make sure that the belt anchor points lie on the same vertical line of the corresponding thigh ones. Figure 2.3

Figure 2.3: Hip exosuit for off-board test. The labels refer to: 1) Elastic belt; 2) Thigh wraps; 3) Cable tendons; 4) Guides to connect the exosuit to the motor device; 5) Upper anchor points; 6) Thigh anchor points; 7) Plastic rings for compliance purposes; 8) Thigh IMUs; 9) Back IMU.

2.2 Software: High-Level Control

The control unit is the set of all the actions that allow to drive the motor in function of the signal coming from the IMUs, according to the periodic movement of the legs. We can distinguish between high-level and low-level modules in the control scheme: the former refers to the steps required to create the reference motion for the motor and includes the kinematic and biomechanical considerations about the walking or running gait patterns, whereas the latter involves the translation of the reference motion into the proper driving command of the system and the communication protocol between the processor and the motor. The control scheme is presented in Figure 2.4.

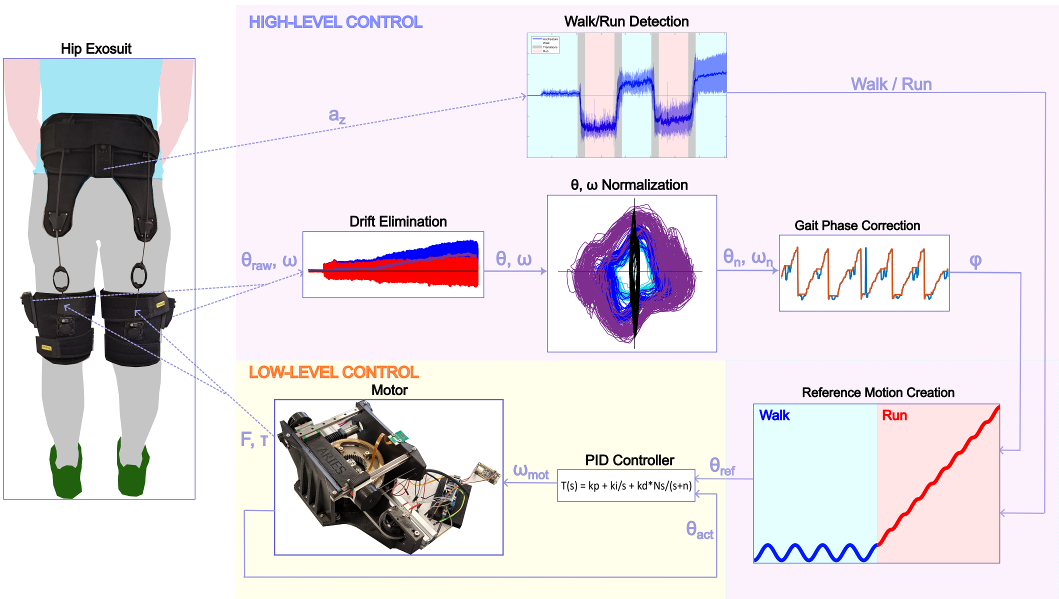

Figure 2.4: Control scheme of the device

The high-level control produces a consistent reference motion in relation to the peculiar characteristics of the motor, starting from purely kinematic data. Two IMUs, one for each leg, are placed on the lateral side of the thighs and acquire the hip angular velocity and angle of the corresponding body segment at a sampling frequency of 100 Hz. The IMUs directly provide the angle values thanks to an embedded algorithm that estimates the orientation of the sensor exploiting the measurement of the accelerometer, gyroscope and magnetometer along the 3 axes (Bosch Sensortec, Reutlingen, Germany). However, since the primary purpose of the exosuit is to assist extension, only the quantities in the sagittal plane are of interest, and there is no concern for the orientation of the legs in the frontal and transversal plane. Therefore, each IMUs only collects the angular velocity of the thigh around the medio-lateral axis and the angle created by the thigh with respect to the vertical axis of the body (which is assumed to be the trunk, with a very good approximation in our case study).

The hip angle and hip angular velocity are derived from the acquired signals. The hip angle is defined as the difference between the right thigh angle and the left thigh angle, while the hip angular velocity (or simply hip velocity or hip speed) is the difference between left and right values to consistently represent the derivative of the hip angle. According to this convention, the hip angle is positive when the right leg is in front of the left leg, getting higher values as the right foot approaches to HS and the left foot approaches to TO, whereas the hip speed is positive when the subject swings the right leg forward and the left leg backward.

2.2.1 Drift Compensation

The computation of the angle by the IMUs is a critical point: it is well known that the direct integration of the angular velocity is not feasible because the gyroscopic measurements are affected by noise and bias, but the algorithms that are embedded into the sensors to reduce the drift also do not display a long-term accuracy which is essential in this field. The drift of the angle is unavoidable and should be minimized. A common solution is to insert additional algorithms, such as Madgwick's or Mahoney's, in cascade to the previous ones to provide a more robust estimation of the orientation of the IMUs. Furthermore, even more accurate approaches based on novel techniques like machine learning schemes have been developed in the last years. On the other hand, they are also quite expensive from a computational point of view with a consequent delay in the system. In the present application, the removal of the drift in a medium- or long-term period is more important than recording a super-accurate value of the hip angle because an error of few degrees has no effect in the behavior of the system. Therefore, in the very first version of the system which will be tested only during straight motion, we decided not to use such algorithms but to implement a much simpler code that adaptively estimates the shift and continuously subtract it from the current angle measurement to prevent its uncontrollable drift.

The right and left thigh angles ranges from about 30° in flexion to about -10° in extension within a stride, but the signal of interest is their difference and it displays a typical sinusoidal pattern over time under the assumption of a quasi-symmetrical behavior of right and left leg. However, this does not occur in real scenarios where the drift affects the two angle measures independently of the other, therefore it is not enough to take the difference of the values.

Our approach is based on the trend of the angle peaks: the drift is modeled as the upward or downward shift of the peak values as the gait evolves. The method adopted to find the peaks is described in details later. Usually, consecutive peaks are slightly different because of the continuous adaptation of our body to the external condition during gait, therefore the shift should not be calculated between two consecutive steps with the same leg but rather considering a set of multiple steps. Moreover, the amplitude of the signal physiologically increases as the person speeds up. As a consequence, looking only at the pattern of the maxima or minima of the angle would lead to a wrong estimation of the drift, so according to the hypothesis of symmetry we decided to track the trend of both positive and negative angle peaks and take the mean of the two shifts.

In real-time applications, techniques like linear regression to estimate the shift are time-consuming and not efficient, therefore the shift is computed simply as the difference between the last peak value and the first peak value of each set of steps with the same leg (according to our convention, the right steps are associated to positive peaks and left steps to negative peaks). With this approach, it is fundamental that the last peak of one group is the first of the following one in order to confine the possible negative effect of such value, for example in case of an abnormal step or of wrong detection of a step, only to a limited time interval. Consequently, the number of steps in each set should be neither too small nor too large: the first in order to reduce the risk of using non-representative peaks, the second in order to avoid the propagation of a negative effect for a long time. Generally, a number of steps in the range 4-7 seems effective in minimizing the drift. During the first steps the subject adapts to the walking or running conditions and the relative peaks are usually not representative of the main gait pattern, therefore the first positive and negative peaks are not included in the computation of the shift. Furthermore, the update of the shift is immediate and causes a jump in the pattern of the value, but it has no effect on the future stages.

Another crucial point is the position of the IMUs: they are not integrated in the structure and any time they are attached to the thigh wraps they may not be perfectly aligned to the vertical axis, introducing an initial offset. To make the inclination of the sensors irrelevant for the control scheme, as soon as the trial starts and the subject is supposed to stand in upright position, the first value of the angle (baseline) is memorized. The shifts deriving from the previous blocks are then added to the baseline, and this value is continuously subtracted to the recording of the angle to obtain the desired pattern.

The outcome of the algorithm is presented in Figure 2.5), where the shift is computed every 4 steps. The long-term effect of the algorithm, instead, is presented in Figure 2.6:

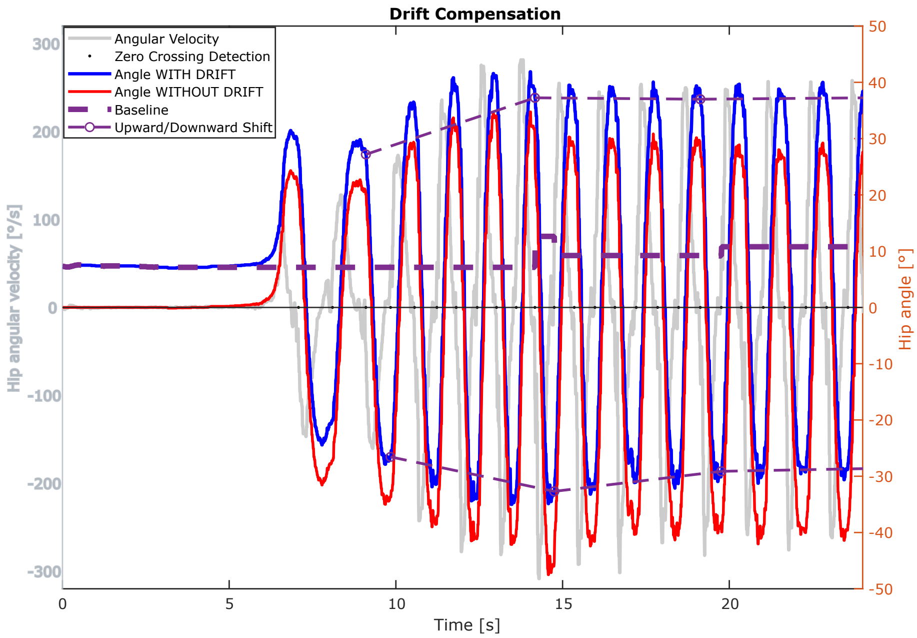

Figure 2.5: Outcome of the algorithm for drift compensation. The baseline is detected at 3s; before that, the subject is allowed to move without any consequence for the system.

2.2.2 Gait Phase

The angular relationship between the hip angle and hip velocity is an indication of the progression of the leg along the gait cycle, the so-called gait phase, and it is the main control variable driving the control framework. Hip angle and velocity are periodic quantities with a sinusoidal trend and the velocity is the derivative of the angle; as a consequence, the two signals are out of phase by

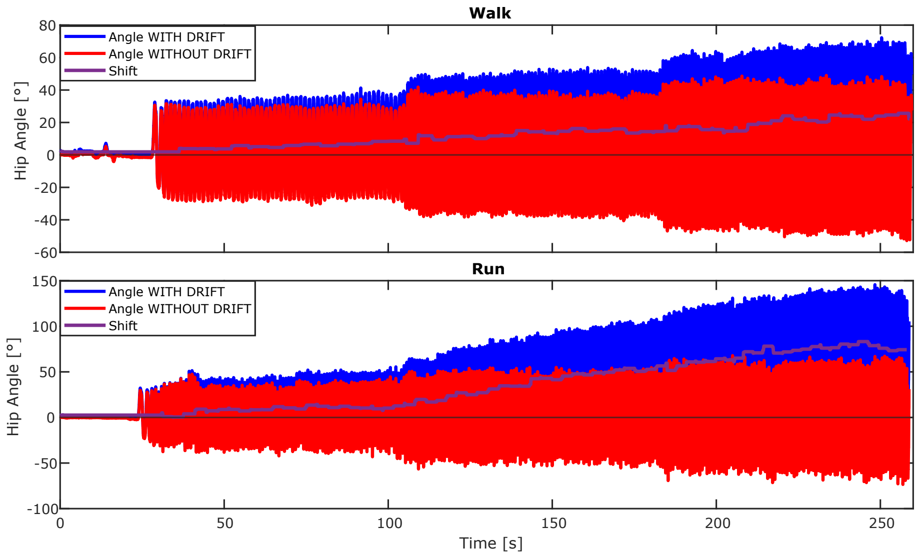

Figure 2.6: Drift compensation while walking (top) and running (bottom) at different speeds.

90° and the gait phase can be seen as the phase angle in the hip phase portrait (velocity vs angle in a polar coordinate system).

Defining the angle as θ(t) and the velocity as $\dot{\theta}$(t) or ω(t), the gait phase can be derived as:

$$\phi(t) = \arctan\left(\frac{\omega(t)}{\theta(t)}\right) \tag{2.4}$$

However, during the gait cycle the hip velocity can be up to 10 times higher than the hip angle, resulting in a phase shift that is not adapt for the development of the reference motion. Hence, the two quantities must be shifted and normalized to obtain a more circular portrait of the hip phase and to enhance the linearity and monotonicity of the gait phase during a cycle [29].

The normalization of hip angle and velocity requires the minimum and maximum values to be stored. This is quite easy in off-line processing, but very delicate in online systems where the peaks cannot be detected automatically. One possible approach is to rely on the derivative of each signal to find the respective peaks: where the derivative crosses zero going upwards, the signal exhibits a negative peak; where the derivative crosses zero going downwards, the signal exhibits a positive peak.

The angle peaks are localized by looking at the velocity, but this is a noisy signal that usually presents multiple zero crossings that lead to an erroneous detection of the features. To overcome this problem, the following steps are implemented:

- Filtering: at this stage the detection of specific events like HS or TO is not important, therefore, even if the frequency content of human walking and running is below 20 Hz, the cut-off frequency can be lowered without any loss of information. On the other hand, a filter with a very low cut-off frequency is computationally expensive and introduces delay, which must be possibly avoided. A cut-off frequency of 60 rad/s (about 10 Hz) has no significant delay on the scheme and efficiently makes the signal smoother.

- Tuning: the previous filtering settings are not able to filter all the spurious zero crossings out; in particular, in correspondence to the correct crossing, the velocity usually displays a sudden change in monotonicity that often leads to a double intersection with the zero line. To by-pass such behavior, the parameters described henceforth are tuned:

  - Threshold: the velocity must cross +0.75 rad/s upwards or -0.75 rad/s downwards (respectively for minima and maxima) to reduce the occurrences of double crossing. Since the velocity increases or decreases very rapidly in this region, the delay is minimal and it affects only the update of the normalization features, not the control process.
  - Angle: when the velocity crosses the corresponding threshold, the angle must be smaller than -10° or greater than 10°, respectively.
  - Time: After a peak occurrence, any detection is disabled for a period of 0.15 seconds. Nilsson and Thorstensson have observed that the maximum human cadence is about 3.57 steps/s at high-frequency run (approximately a step every 0.28 seconds) [30], whereas professional sprinters even reached a step frequency of about 4.5 steps/s (approximately a step every 0.22 seconds) so the selected value is appropriate for step detection. This further prevents from a wrong detection when the velocity presents large fluctuations.
  - Alternation: there are separate blocks for the detection maxima and minima because of the drift elimination algorithm. After recognizing a maximum, the system expects a minimum, therefore the block of the latest detected feature is disabled, with the additional intention to reduce the computational weight of the scheme. The two blocks

are simultaneously active only at the beginning of the trial to be prepared for the detection of whatever step as first step.

The detection of velocity peaks is much simpler as we can simply look at the angle: with the assumption of sinusoidal behavior, the second derivative of the angle, which is the angular acceleration (derivative of the velocity), is the same signal with a negative constant of proportionality. In particular, the zero-crossing points are the same, therefore a downward zero-crossing of the angle corresponds to a negative velocity peak, whereas an upward zero-crossing corresponds to a positive peak. The strategy is reversed from that of the angle detection. This method allows to avoid the numerical computation of the acceleration which is expensive, inaccurate and noisy, and does not need any other check because the angle does not display any fluctuation, especially near the intersection with the zero line.

At each time instant, the normalized angle and velocity signals are constructed upon the latest peaks:

$$\begin{aligned} z(t) &= \left| \frac{\omega_{max}(t) - \omega_{min}(t)}{\theta_{max}(t) - \theta_{min}(t)} \right| \\ \gamma(t) &= -\frac{\theta_{max}(t) + \theta_{min}(t)}{2} \\ \Gamma(t) &= -\frac{\omega_{max}(t) + \omega_{min}(t)}{2}. \end{aligned} \tag{2.5}$$

where z(t) is the scale parameter and γ(t) and Γ(t) are the shift parameters calculated from the filtered thigh angle and velocity, respectively. From 2.5, the normalized variables are obtained:

$$\theta_n(t) = z(t) \cdot (\theta(t) + \gamma(t)) \tag{2.6}$$

$$\omega_n(t) = -(\omega(t) + \Gamma(t)). \tag{2.7}$$

and the gait phase from 2.4 becomes

$$\phi(t) = atan2\left(\frac{\omega_n(t)}{\theta_n(t)}\right) \tag{2.8}$$

The function atan2, unlike atan, computes the phase angle taking into account the four quadrants and returns a value in the range $[-\pi, \pi]$. The negation of

$\omega_n(t)$ in (Equation 2.7) ensures that the phase portrait of the hip angle orbits in a counter clockwise direction (Figure 2.7.a)

Due to the imperfections of the velocity trend, the phase shows some small negative peaks which must be eliminated to make it monotonously increasing inside the gait cycle. Hence, any time the signal has a negative derivative, the system stores the value of the latest maximum peak and the phase maintains that constant value until the signal becomes higher (Figure 2.7.b)

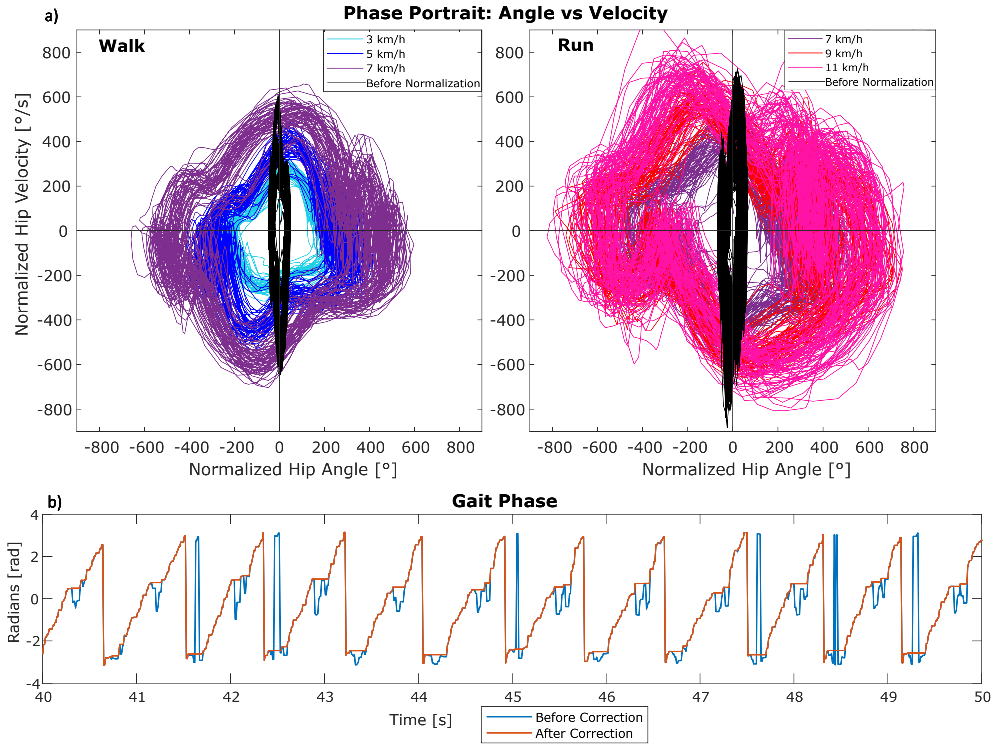

Figure 2.7: a) Phase Portrait before and after normalization. b) Evolution of phase over time: the red signal is the phase after both normalization and elimination of negative peaks

The hip angle has a sinusoidal behavior that can be well approximated with the sine of the gait phase (SGP). This signal is normalized in the range [-1,1] and it is also optimal to track the future reference position of the motor because of the peculiar characteristics of the device. Finally, a linear Kalman Filter eliminates the constant sections appeared in the previous step and makes the sinusoidal signal smoother, despite introducing a delay of few samples.

In parallel to the gait phase, other gait parameters are computed. The step time is defined as the interval of time between two consecutive hip angle peaks, and it is expressed in seconds. Due to the little asymmetry in the velocity trend between the two legs and to the noise that may affect the accuracy of detection, the right steps are usually systematically different from the left steps, resulting in a square wave pattern. For that reason, the system takes the average of two consecutive step times and provides a more regular pattern of the measure over time. The instantaneous cadence (the reciprocal of the step time), the leg associated to the last step and the number of steps since the beginning of the trial are also obtained. In addition, the system also calculates the evolution of the step cycle percentage: it is computed as the ratio between the time from the beginning of the current step and the duration of the previous step, expressed in percentage as explained in Eq. 2.9. The step cycle percentage starts from 0% at the detection and then progressively increases. If the current step lasts more than the previous one, the step cycle in the corresponding samples is saturated at the maximum value of 100%. Except the step cycle percentage, all these features are calculated at each hip angle peak and remain constant for the entire duration of the present step.

$$g(t) = \min\left(1\ ; \frac{t - t_s}{t_s - t_{s-1}}\right) \cdot 100\% \tag{2.9}$$

where t is the current time instant and s is the current step number.

2.2.3 Walking/Running Detection

The ability of determining the current locomotion mode of the subject in real-time is one of the key features of the exosuit. Not only does it make the motor switch from one modality to the other, but it also allows to provide the correct assistance profile which is tailored based on the different timings of the gait events during the gait cycle.

Walking and running are different from kinematic and kinetic perspectives and can be investigated using a moltitude of sensors. However, as it often happens, their identification during online settings becomes arduous, especially when few data sources are available as well as a limited computational power.

The clearest dissimilarity between the two activities is the presence or absence of flight phases and double support phases. Determining if flight phases exist requires the reliable detection of HS and TO events for both feet. Unfortunately, catching these gait events in a reliable and robust way is a challenging task, especially in case of very short flight time intervals. Foot-mounted sensors, like insoles, would be needed for this purpose, with the drawback of increasing the complexity of the system.

The same reason prevents from focusing on the knee joint angle. At mid-stance, the knee is relatively straight during walking but flexed during running. However, the knee angle can only be determined with the introduction of two more IMUs, placed on the lateral side of the shank for each leg. In fact, it is defined as the angle between the thigh segment and the shank segment and can be extracted as the difference between the real-time thigh IMU angle in the sagittal plane and the corresponding shank IMU angle. This means a total of 4 sensors in the structure that can also affect the physiological movement, since they all must be placed firmly on the legs of the user.

The whole high-level control layer requires just one IMU on each leg for the creation of the reference motor command, which makes the structure modulable and compact. With the intention to not introduce more sensors, we tried to develop a strategy to discriminate walking from running using the same two IMUs placed on the side of the thighs. Moreover, no machine learning techniques were taken into consideration with the purpose to reduce the system delay and to not introduce additional computational devices on the structure.

This methodology starts from considerations about the linear speed of motion. As reported in 1.1.2, the transition between walking and running usually takes place spontaneously when the person speeds up and exceeds a velocity threshold, in correspondence to which the Froude Number becomes higher than 1. However, this is just an indication and hardly can be traduced in a useful information for the control system: there is a range of intermediate velocities, usually between 5 km/h and 8 km/h (but it changes from subject to subject), where people are able both to walk and run and can decide how to move depending on the specific situation. In particular, at those speeds humans either walk faster or run more slowly than a walking or running activity at self-selected speed, with the further possibility to modify their traditional and physiological motion. Hence, the subject's motion must be properly investigated.

During both walking and running, an increment in velocity is always followed by higher step frequencies and step lengths, which can be translated into IMU quantities in terms of larger hip angles and hip angular velocities inside each stride. We based our attempt on the evaluation of the trend of these kinematic features as the velocity increases.

Normally, the maximum hip angle is higher during walking than in running at the same linear speed. This happens because the walker swings the straight leg forward with more effort to cover the same distance, causing a longer step length and a lower cadence with respect to running, while the runner pushes vigorously onto the ground to complete the step without the need of flexing the forward leg as much as during walking. On the other side, at high speeds the runner shows a big flexion of the forward leg before starting the propulsive phase, bringing the thigh closer to the trunk and reaching larger hip angle than those in walking. As a consequence, looking just at the entity of the peak of the hip angle does not allow to distinguish the two activities. Similarly, we cannot use only the maximum hip angular velocity over a step, because these features have overlapped distributions for walking and running.

Nevertheless, hip angle and angular velocity peaks are almost never equal in walking and running at the same speed. Therefore, an opportunity is to express the kinematic quantities of interest in function of the subject's velocity: if the two trends are different and they never intersect in proximity of the range of intermediate speeds, then the specific motion can be determined by combining the two pieces of information.

At this point, however, there is a huge barrier to face: with IMUs is not possible to obtain a reliable measure of the subject's linear speed. As it happens with the estimation of the angle, the integration of the noisy data from the sensors creates a totally unreliable signal that diverges from the expected outcome; even more hazardous would be a double integration of the acceleration along the antero-posterior direction to extract the position. There exist methods to estimate the gait speed, but they either exploit machine learning models [31] or require additional sensors on the shank [32] [33]. In particular, the latter approaches are based on the assumption that the leg perfectly rotates around the ankle joint during the stance phase, so the parameters can be obtained according to the inverted-pendulum model. These techniques involve the integration of linear acceleration and angular velocity in the sagittal plane to determine the orientation of the IMU and the spatial gait parameters. Such operation has a good accuracy when the integration restarts at each occurrence of a specific gait event (usually the shank vertical event, when the shank is perpendicular to the ground) to make the unavoidable error affect only the corresponding step and to prevent its accumulation. Still, this approach works mainly offline because of the limited precision in the real-time identification of specific gait events and all the issues related to the integration procedures are amplified in online applications.

With the employment of only two IMUs attached to the thigh, the previous algorithm cannot be applied: the thigh is not integral with the ankle axis of rotation, so the conversion from hip kinematics to linear speed would require also information about the dynamics of the shank, recalling the need of additional sensors. On the other side, the inverted-pendulum model can be extended to the entire leg when describing the walking dynamics, because the leg is relatively straight during the stance phase and the hypothesis of the thigh rotating around the ankle joint becomes meaningful. Therefore, not only can the linear speed be properly estimated during walking, but it can also be done in real-time without any integration.

The velocity is computed as the mean linear velocity inside each step, updated at every step detection. By definition, it is the ratio between step length and step time. While the step time is the time interval between hip angle peaks, the step length is estimated as follows: since the leg is straight during stance, the step length can be seen as the projection of the leg onto the ground across the entire step. The maximum left and right hip angle increases together with the speed, unlike the angle in extension that is regularly about 10°. Considering that the single angle measurement is affected by drift and cannot be directly used, the range of motion during flexion is obtained as half the difference between the hip angle peak of the last right and left step (the left peak is negative, hence the resulting value is positive), called Θ. Actually, remembering that the hip angle is defined as the difference between the angles of the two thigh segments, this method overestimates the angle in flexion because it has the contribution of the contralateral leg which is in extension at the moment of the hip peak. The final formula is reported, where the first term refers to the range of motion during flexion and the second refers to extension. The leg length l is estimated from anthropometric tables as $l = 0.53\ H$, where H is the person's height.

$$length_{step} = l \cdot (\sin\Theta + \sin 10) \tag{2.10}$$

$$vel_{step} = \frac{length_{step}}{time_{step}} \tag{2.11}$$

According to the human walking kinematics, this relation can be adopted to derive the walking linear speed. But is this also practicable for running? Running cannot be described with the inverted-pendulum model because of the different energy profile inside the gait cycle. In particular, the presence of the flight phase and the flexion of the knee during the swing phase makes the association between step length and projection of the leg onto the ground inconsistent. It is still necessary to investigate both locomotion modes with the same approach, without any a priori distinction. Therefore, a quantification of the discrepancy between the actual subject's speed and its estimate using the aforementioned method can reveal how far it is from describing this aspect of the running kinematics properly.

A small experiment was conducted on 4 subjects. They had to walk and run at different speeds on the treadmill while the high-level control section developed the real-time estimated velocity, updated at each step. Each walking trial lasted 6 minutes, during which subjects changed speed every minute and they went from 3 to 8 km/h; in the same way, they run from 5 to 9 km/h, for a total of 5 minutes. Only 45 seconds of each fraction have been actually analyzed, to exclude the transitions between speeds. The purpose was to specifically assess the behaviors at intermediate velocities.

The results are presented in Figure 2.8. As expected, the algorithm shows a better accuracy in the speed estimation while walking due to the closer match to the inverted-pendulum model. Both trends grow slower than the treadmill velocity does: the faster the person moves, the stronger the underestimation of the real speed. At low-speed walking, the scheme actually highlights an overestimation of 12% which gradually disappears at about 5km/h until reaching an underestimation of about -6% at the maximum walking speed. On the other side, in running the algorithm always provides a lower speed value than the actual one, with an initial gap of -14% that increases up to about -24% at 9 km/h. The estimate of the same speed across subjects fluctuates more in running compared to walking. Another detail is that the estimation of the running speed at 9km/h is just above the result of the algorithm for the 7 km/h walking fraction: this means that the estimated value falls in the range of intermediate speeds even when the subject runs at higher paces. As a consequence, the running velocity should be much higher to obtain an estimate that is greater than a threshold and that allows to automatically exclude the probability of walking.

On the other side, the trends of estimate values for each subject can be well described by a regression line in both activities, as presented in Figure 2.9, with a coefficient of determination which is always above 0.98 in walking (above 0.998 for three subjects) and above 0.90 in running (above 0.97 in three of them). This reflects a regular increase in the speed estimation between consequent fractions and a standard behavior of the algorithm throughout the trial. At this point, the relationship between the angle peak and the estimated speed must be analyzed to see whether the walking and running profiles have superimposed or distinct

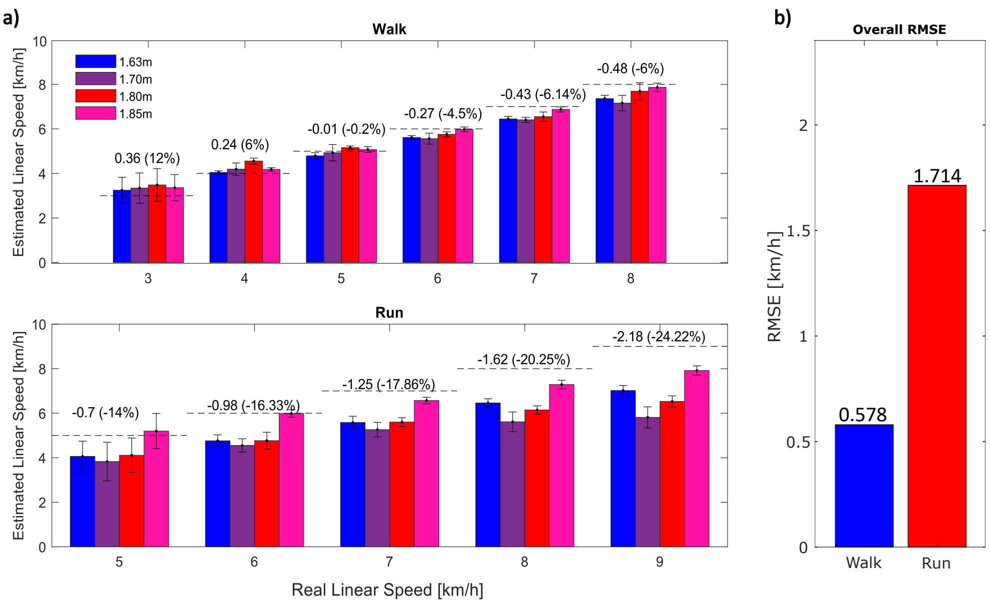

Figure 2.8: a) Estimate of linear speed for all subjects. The real speed is showed as a dashed horizontal line. The gap between the average estimate of the speed and the real speed is reported as value and as percentage. b) Overall RMSE of the estimation of the linear speed.

distributions.

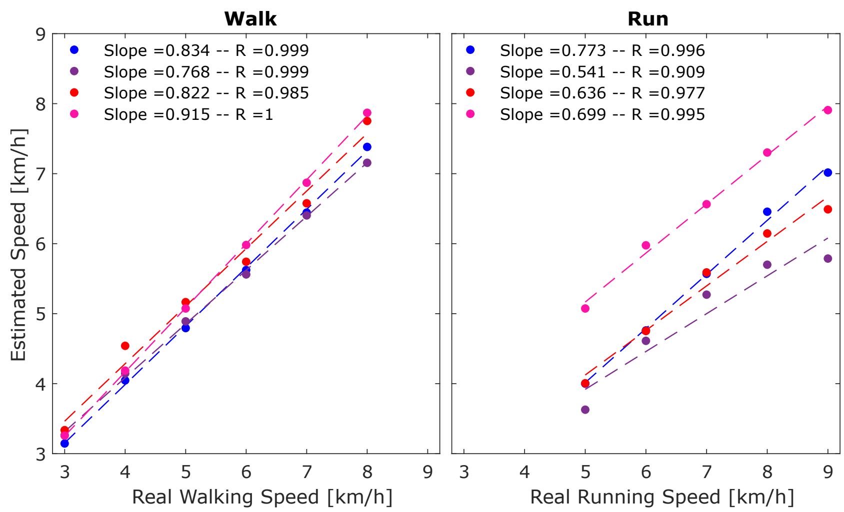

Figure 2.9: Trend of the estimate of the linear speed in function of the real speed for each subject. The angular coefficient of each line and the coefficient of determination for each comparison are reported.

Figure 2.10 presents the trends of the median value of the angle peak in function of the estimated speed. In 3 out of 4 subjects, the two trends are completely separated in correspondence of the range of intermediate speeds. It means that the feature has a relevant difference from walking to running for each speed, even if the process of estimation is not accurate enough. A threshold line between the two trends can be identified: it is the regression line that interpolates all the points created as average between data points of one locomotion mode and their vertical projection on the line corresponding to the other locomotion mode. Walking or running are recognized depending on the value of the hip angle falling above or below the threshold, respectively, for the real-time estimated velocity.

A further check is about the distance between the two trends, Δ. The threshold line lies exactly at halfway, but a smaller margin of tolerance equal to $1 \cdot \Delta/6$ is implemented to avoid frequent switching. Therefore, the actual threshold is always at least $2 \cdot \Delta/3$ far from the regression line of the currently active locomotion mode. Such value is compared to the maximum standard deviation of the hip angle peak for different speeds: if the standard deviation of the peak data for each speed is too large, and specifically larger than $2 \cdot \Delta/3$, the values fluctuate more and the probability of a value lying on the wrong side of the threshold line increases. In two subjects out of four, the distance between trends is enough to theoretically prevent from wrong detection, while a subject reported an higher standard deviation than the threshold, which reduces the robustness of the algorithm. On the other side, the trends of subject 1 meet in correspondence of an estimated speed of 8 km/h: this means that there is no margin of tolerance and that the discrimination between activities at this speed is unreliable.

The drawbacks of the 2-IMUs method led to the decision of investigating the dissimilarities between walking and running from another perspective: the profile of the potential and kinetic energy of the COM in a step cycle (a dynamic criterion). As previously explained, in correspondence to the maximum extension of one leg (that is almost simultaneous to the HS) the COM reaches the lowest point of the profile during walking, but the highest point during running. Consequently, the gravitational potential energy of the COM, that is linearly associated to the height, is minimal at HS during walking and maximal during running. The exclusive use of IMUs does not allow to track the vertical position of the COM, because the double integration of the acceleration is not a feasible option due to the noise within the measure. However, the COM describes a sinusoidal movement over time, so the vertical position and the acceleration, its

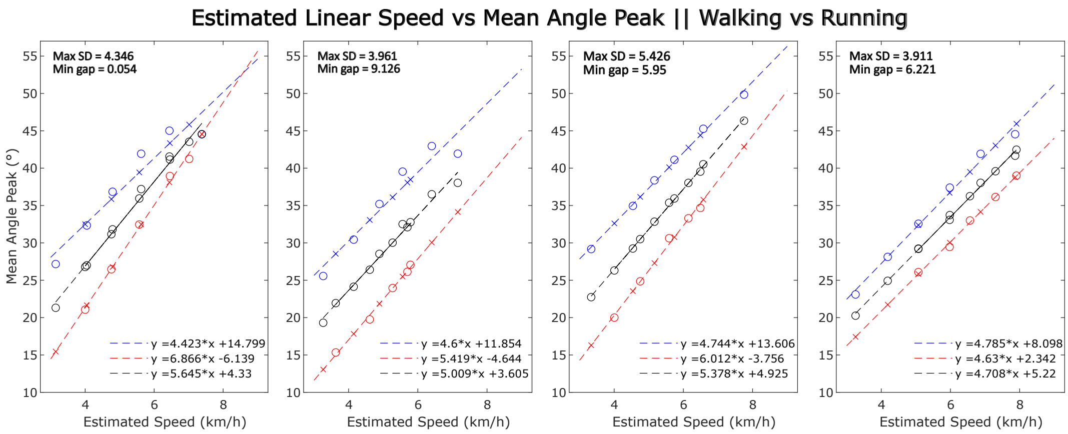

Figure 2.10: Trends of mean angle peak in function of the average estimated linear speed for each real speed, for walking (blue) and running (red). The black line is the threshold to discriminate the two locomotion modes. The o are the actual data points for the corresponding mode, while the x points are created by projecting vertically the actual points for each mode onto the other mode's line. The maximum standard deviation of the angle peak among all speeds is reported and compared with the minimum vertical distance between the two regression lines.

second derivative, have the same sinusoidal trend but shifted of 180° (or times a negative constant of proportionality). This means that at HS the acceleration is expected to be positive for walking and negative for running. Therefore, by looking at the acceleration profile it is possible to determine if the subject is walking or running.

A third IMU is necessary to monitor the trend of the acceleration of the COM. Despite the need of an additional sensor, it is still a smaller requirement than those of other kinematic approaches for the detection, and its location (on the back in correspondence to L5, as close as possible to the real COM position) does not affect the subject's motion at all. Only the vertical acceleration is meaningful for the purpose and the trunk is assumed to be always aligned with the vertical axis; in this case it is fundamental to orient the IMU correctly.

The noisy acceleration signal is originally filtered at about 10 Hz (no delay introduced) and then segmented, taking the strategy of Kim et al. [25] as inspiration. The maximum extension is intended as a stage of gait cycle rather than a single event: it is defined as the interval between 90% and 15% of the step cycle percentage. For each step, the mean of the acceleration inside this interval is computed and then used as feature to discern the two locomotion modes. According to the kinematics and based on simulations, there is almost no overlap in the distributions of this feature for walking and running, hence a heuristic classifier can simply rely on thresholding feature value to classify each step as either walking or running gait.

In theory, a threshold of $0\,m/s^2$ can be used, but a small tolerance margin has been implemented to increase reliability. We used a threshold of $\pm 1.5\,m/s^2$: walking is detected if the mean of acceleration is above $+1.5\,m/s^2$, running is detected if it is below $-1.5\,m/s^2$. If the feature is between the two threshold values, the system remains in the current locomotion mode. Moreover, in order to avoid false and frequent switching, the algorithm was designed to check that the feature is above (or below for walk-to-run transition) a given threshold for at least two consecutive steps before triggering a run-to-walk (or walk-to-run) transition. Only if the feature value changes from a strongly negative to a strongly positive value (or vice-versa) the controller allows a fast single-step transition from one gait mode to the other. The algorithm for walking or running discrimination has been implemented with a state machine strategy, which is presented in Figure 2.11.

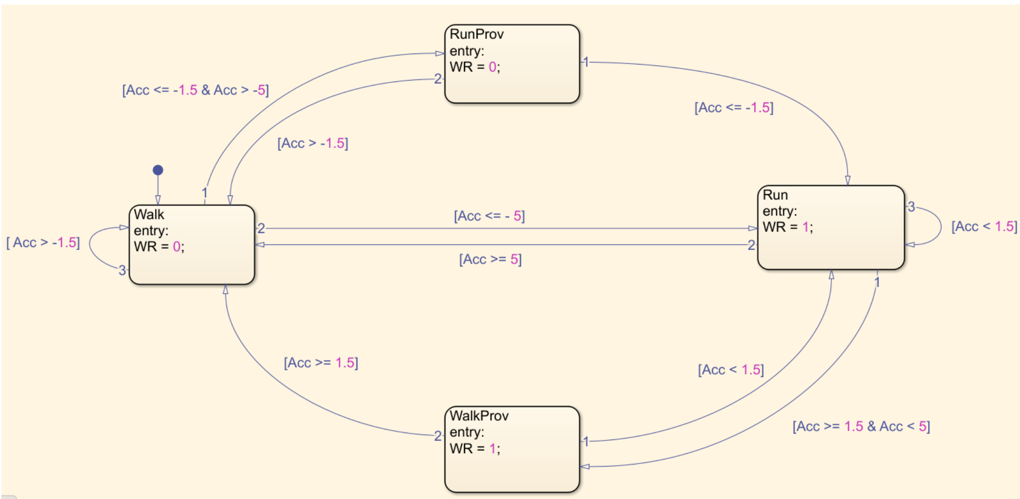

Figure 2.11: State-machine algorithm to discriminate walking (WR = 0) from running (WR = 1), based on acceleration feature (Acc).

Both algorithms were tested in parallel to quantify their accuracy in the recognition of the real locomotion mode and to choose which one to adopt in the following stages. The same four subjects had to complete a mixed walking/running trial on the treadmill, consisting of 5 consecutive sections of 75 seconds each:

- 3 km/h Walking;

- 7 km/h Running;
- 7 km/h Walking;
- 11 km/h Running;
- 5 km/h Walking;

Each subject was tested on his/her own model during the assessment of the goodness of the 2-IMU method. Only the performance of the algorithm in the middle of each section is of interest at this stage, therefore the transitions between speeds are excluded from the evaluation and just 60 seconds of each speed are actually analyzed. The subjects are equipped with a belt that carries the IMU on the correct position on the back and, being connected with the thigh IMUs, prevents their sliding down during the trial.

The results in Figure 2.12 show a superiority of the 3-IMU method, with an overall accuracy of 97.54% against 87.81% of the 2-IMU method. Interestingly, the difference in the performance of the algorithms is related to those subjects that previously displayed faulty trends in their models: the accuracy of the 2-IMU method drops to 77.4% and 77.1% and it is due to a wrong detection during running at 11 km/h, in correspondence to which the estimation of the running speed is less accurate and the walking and running regression lines get closer to each other.

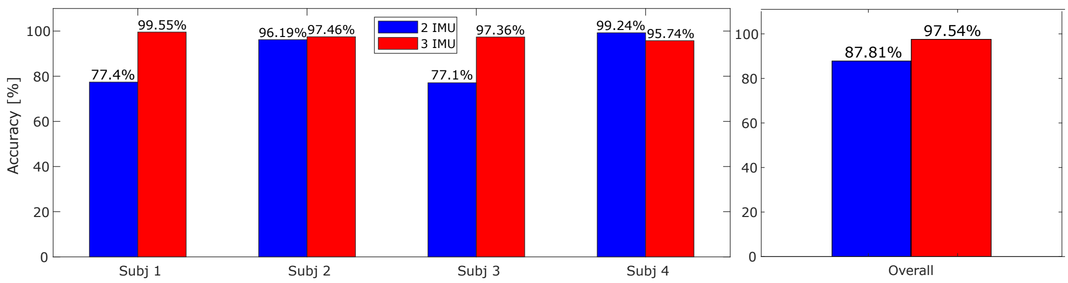

Figure 2.12: Accuracy of the two methods to discriminate between walking and running

Following these results, I chose the 3-IMU method for the real-time discrimination of the locomotion mode. The main advantage of this approach is that it does not require any tuning or adaptation to the subjects' anthropometry because the profile of the acceleration of the COM is common to all healthy people, so the threshold is generally valid. Moreover, the use of a third IMU on the back does not increase the complexity of the system: the IMU itself is very lightweight and simply attached to the belt, which is an intrinsic part of the exosuit, and the introduction of an additional signal does not deteriorate the stream of data via Bluetooth.

2.2.4 Creation of the Reference Motion

The reference position of the motor can be generated following multiple approaches. Many exosuits are equipped with load cells or force sensors, so the development of the reference command for the motor is usually based on the quantification of the desired force or torque that must be applied to the hip joint. However, it often results difficult to close the control loop accurately due to the characteristics of the kinetic signal. A valid alternative is to derive the reference position indirectly from kinematic variables: beside the advantage of not using other sensors than the two IMUs on the thighs, it allows to model the desired command on a normalized signal, which is independent of the user.

Our scheme follows the latter strategy, where the reference signal is tuned on the basis of the SGP. This signal has ideal properties: it is sinusoidal and normalized between -1 and 1 (perfect for the alternation between legs) and its frequency is the same of the subject's cadence. The extension of each leg is associated either to the rising or falling section of the SGP: the mononicity of this signal is well preserved inside each interval, therefore each cycle of assistance can be easily identified between two consecutive zero-crossings of the derivative of the SGP.

As described in the hardware section, the motor design allows to make it spin continuously while maintaining a limited amount of cable to provide to the user. At low speeds this is not essential, but when the subject speeds up a traditional motor would be forced to reverse the direction repetitively and it would not be able to follow the input command, leading to an ineffective or even dangerous assistance. Accordingly, we decided to split the behavior of the motor: when the user walks the device alternates its direction of rotation, otherwise it keeps spinning in the same direction to avoid all the inertia-related problems.

The general profile of assistance is characterized by a half-rotation of the motor: the motor assists the extension of one leg by driving the linear output from one extremity to the other. Following our convention, the motor rotates from 0° to 180° to support the right leg, corresponding to a shift from the bottom to the top boundary of the linear output, while to support the left leg it rotates from 180° to 0° or 360° depending on the modality of rotation, and the linear encoder shifts from the top to the bottom extremity.

The *alternation* mode is characterized by a repetitive movement of the motor back and forth between the two extremities. The motor follows the same trend of the SGP (except for the tuning parameters) and rotates from 0° to 180° and then back to 0° to assist an entire gait cycle. The motor enters this modality when walking is detected.

As soon as run is detected, the motor shifts to the *rotation* mode: after assisting the right leg and reaching the position of 180°, the motor keeps the same direction of rotation and assists the left leg going from 180° to 360°. At this point, if the motor is given a command to rotate from 0° to 180° (corresponding to the right leg), the reference motion would shift abruptly from 360° to 0° causing one rapid complete rotation of the motor in the opposite direction. To avoid this and to guarantee continuity across consecutive cycles, any time the motor reaches a position which is multiple of 360° the system stores that value and adds it to the following reference motion. In other words, if this behavior is preserved, the system adds an offset of 360° to the reference motion every time the assistance to the left leg is over. Moreover, as soon as the motor enters this modality it keeps rotating in the same direction as in the last assistive cycle during *alternation* mode; consequently, if the right leg was the last one to be assisted before the switch, the motor rotates towards more positive position values, otherwise it rotates towards more negative values.

When a run-to-walk transition is detected, the motor comes back to the *alternation* but the new reference motion is limited in the range [0°; 180°] plus the latest offset.

Prior to the accurate tuning, the reference position in *alternation* mode can be described by Eq 2.12:

$$\theta_{alt} = (-sin(\phi) + 1) \cdot 90 + q \tag{2.12}$$

while in *rotation* mode it follows:

$$\theta_{rot} = \begin{cases} (-sin(\phi) + 1) \cdot 90 + n \cdot 360 + q & if \frac{d}{dGP}(-sin(\phi)) \geq 0 \\ (sin(\phi) + 3) \cdot 90 + n \cdot 360 + q & if \frac{d}{dGP}(-sin(\phi)) < 0 \end{cases} \tag{2.13}$$

where n is the number of minima of $-sin(\phi)$ detected since the beginning of the trial in rotation mode exclusively, whereas q is the offset, which is updated only when the transition between *rotation* and *alternation* takes place:

$$q = \lfloor \frac{\theta_{rotfin}}{360} \rceil \cdot 360 \tag{2.14}$$

A simple example of the reference motion before the tuning procedure is showed in Figure 2.13.

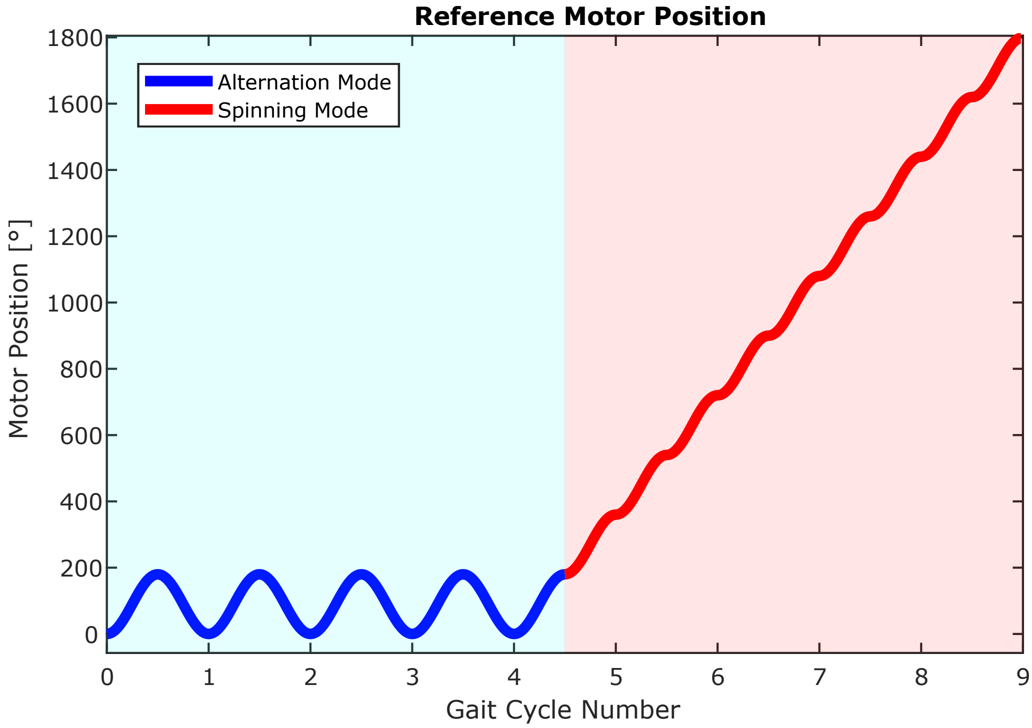

Figure 2.13: Reference motor position in walking and running before tuning

The tuning of reference motion is essential to reduce the effort of hip muscles during extension. The resulting torque profile of the motor should have the same shape of the physiological hip torque profile in the sagittal plane (Figure Figure 2.14).

The hip torque during extension has a Gaussian-like profile that starts at approximately 85% of a gait cycle and terminates at 20% of the following cycle for walking, while in running the profile is slightly anticipated (from 80% to 10% of a gait cycle) and reaches more limited values. The gait cycle is defined between two consecutive HS. However, in our algorithm the beginning and end

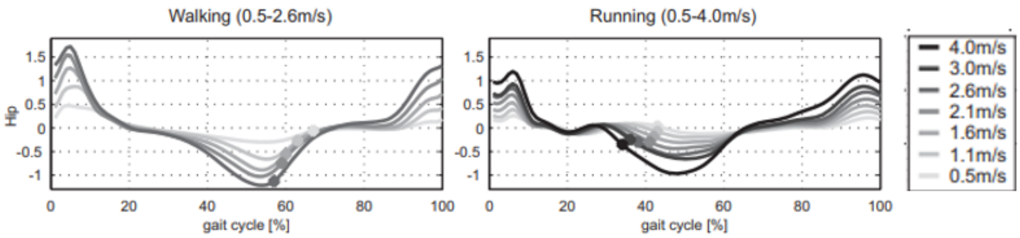

Figure 2.14: Hip torques at different speeds [34].

of the steps are identified by the peaks in the hip angle trend. As a consequence, it is necessary to investigate the succession of gait events inside a cycle to make our profile consistent.

In real-time scenarios the identification of the HS using two IMUs is not accurate, but through the separate investigation of right and left thigh angle trends it is possible to highlight the timing of maximum extension and flexion of each leg. This analysis was made on 3 subjects during a walking (at 3, 5 and 7 km/h) and a running (at 7, 9 and 11 km/h) trial; each speed was evaluated in an interval of 60 s. In Figure 2.15 the single thigh angles, their difference (hip angle) and all features are presented, from which important qualitative information can be extracted:

- The maximum flexion of one leg is not simultaneous to the maximum flexion of the other leg. The sequence of events is Extension R - Flexion R - Extension L - Flexion L - Extension R and so on, which remarks the sequence of TO R - HS R - TO L - HS L - TO R but at different timings;
- The angle peak usually occurs between the maximum flexion of one leg and the extension of the other;
- When the hip angle is zero, not necessarily are the two thigh perfectly aligned with the vertical axis.

A further quantitative analysis based on events inside a step cycle (and not inside a gait cycle), Figure 2.16, shows that:

- In walking, the maximum flexion occurs at about 80%, the maximum extension at about 5% and the zero hip angle at 43%, which, if converted to gait cycle percentage, are about 90%, 3% and 22%, respectively;

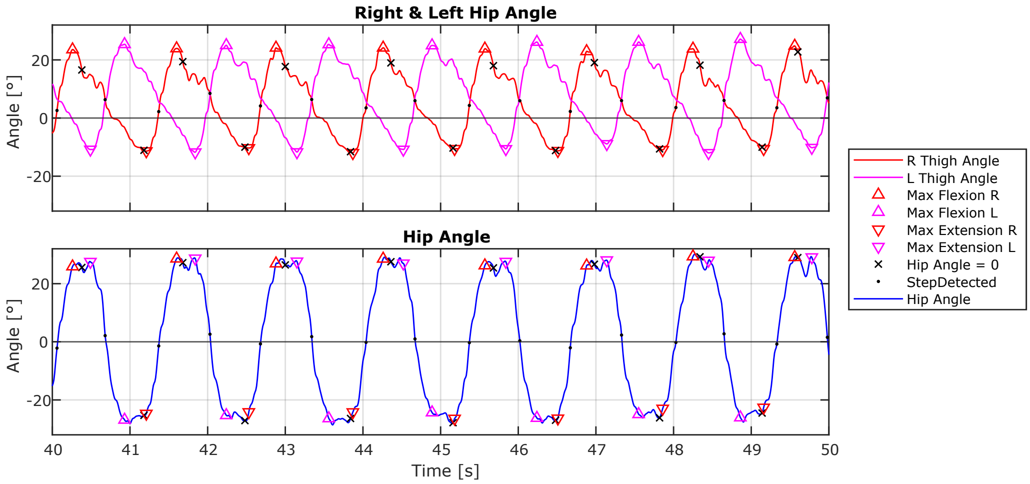

Figure 2.15: Example of single thigh angles and hip angle with all relevant gait events

- In running the maximum flexion occurs at about 86%, the maximum extension at about 4% and the zero hip angle at 57%, which, if converted to gait cycle percentage, are about 93%, 2% and 28%, respectively.

The values of walking seem concordant with those of Figure 2.14; this means that the HS and the peak of the hip angle are almost simultaneous. Therefore, the useful action from the motor should start in correspondence to the maximum flexion of the forward leg and terminate approximately when the hip angle drops to zero. On the other side, while the subject is running, the assistance should begin slightly before the maximum flexion of the forward leg and expire before the hip angle goes to zero. Moreover, the maximum flexion of the leg occurs later in the gait cycle as the speed increases, both in walking and in running. This also occurs for the zero hip angle event during walking, while the other variables display a trend that seems independent of the subject's speed.

The previous analysis shows that the peaks of the hip angle must be in the middle of the profile of assistance, hence the step detection cannot be simultaneous to the beginning or end of the profile of assistance. The gait features (such as step time, step counter, cadence, etc.) are calculated at the end of each step, but the values that feed the block for the creation of the reference motion are updated only at the end of each cycle of assistance: this prevents from any unexpected behavior of the motor, especially when a transition between different modalities takes place.

Based on these pieces of information, the final reference position is obtained

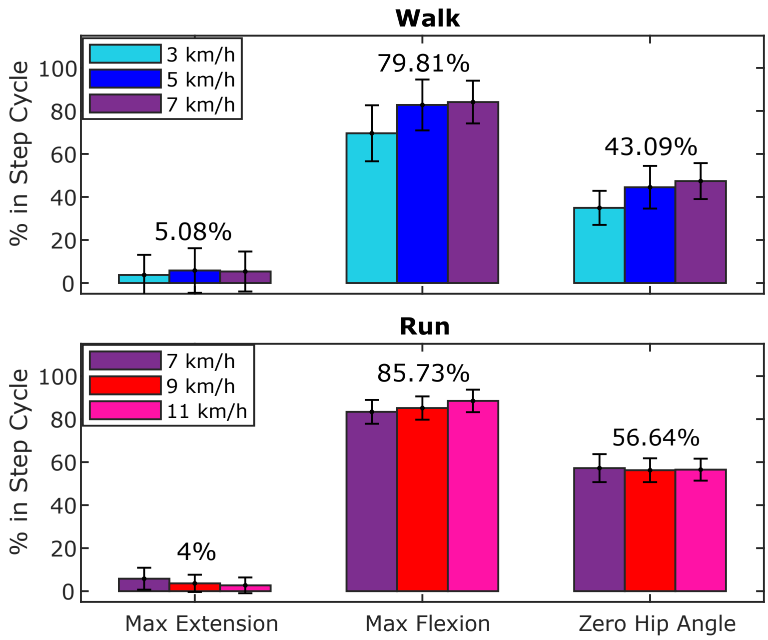

Figure 2.16: Occurrences of gait events inside a step cycle for walking and running

and presented in Figure 2.17. The linear position of the guide is the intended output of this tuning process and its concrete motion is indeed confined in the desired portion of the step cycle, from maximum flexion of forward leg (before the maximum hip angle) to the zero hip angle. It can be observed that, despite the linear output is almost stationary at the two extremities, the motor is still in action: there is a range of almost 30° in the motor rotation in correspondence to which the position of the linear output is basically constant and this marks a break from two consecutive cycles of assistance.

2.2.5 Correction of Initial Steps

Every cycle of assistance is associated to a half-rotation of the motor, with a consequent shift of the linear output from one extremity of the device to the other. When the subject is already in motion, the reference motion depends on the SGP and takes its characteristic trend over time. On the other side, when the user starts walking the gait phase is not computed or is quite unreliable because its creation requires the normalization of the angle and the velocity, which takes 2 or 3 steps. Therefore, the first steps are critical and need a

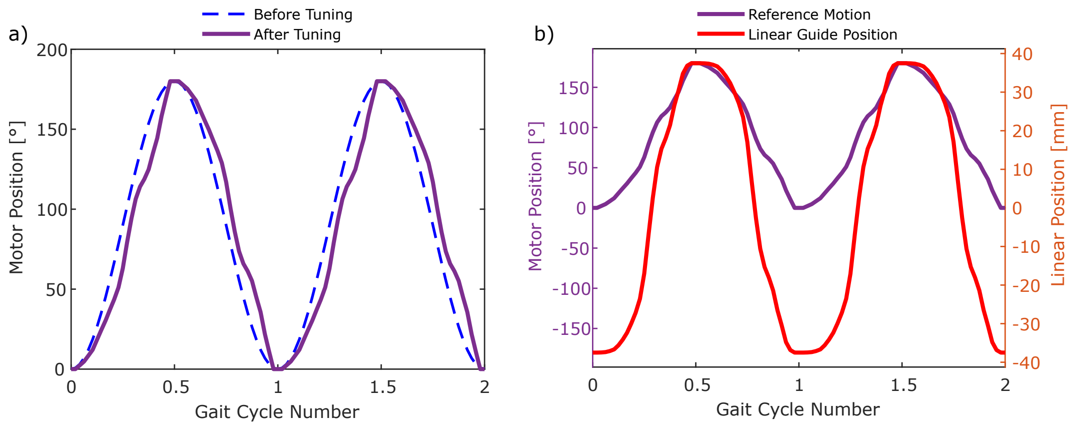

Figure 2.17: a) Reference command position before and after tuning; b) Reference command position and the relative linear guide position

tailored profile of assistance.

At the beginning of the trial, the person is in standing position and free to choose which leg to move forward first. Accordingly, the device must be able to support both legs depending on the decision, hence the motor must start at 90° - the default position - where the linear output is in the middle of the range. When the subjects swings the first leg forward, the controller recognizes the intention as soon as $|hipangle| > 15^{\circ}$ and gradually drives the motor to the corresponding extremity: in 0.12 seconds the position of the motor linearly varies from 90° to 0° or 180°. This happens before the detection of the first step. After that, the motor must span 180° in the other direction. At the moment of the first step detection, the motor should have already started rotating because of the previous considerations about the timing of the profile of assistance; moreover, the SGP is still unusable, therefore the reference motion is modeled as a curve that shifts from 180° to 0° (or viceversa) with the same rate of the angle profile during its transition from the peak value to zero. At the end of the second cycle of assistance, according to our convention about the steps, the SGP may or not be fully developed: if the subject started walking with the left leg, the reference motion for the current step is created as for the previous one, whereas if the subject started with the right leg, the reference motion is modeled upon the SGP. After that, the entire gait cycle can be assessed only by relying on the SGP without further manual settings.

2.2.6 Stop Detection

The normalization of hip angle and angular velocity for the enhancement of the linearity and monotonicity of the gait phase inside a gait cycle creates a circular phase portrait. The polar radius of the portrait, computed as $r(t) = \sqrt{\theta_n(t)^2 + \omega_n(t)^2}$, has a linear correlation to the subject's gait speed as reported in [29]. This method does not allow to provide a very accurate estimate of the linear speed, especially because different subjects can display various phase portraits with slightly different regression lines, but can be effective in detecting when the subject instantly stops walking. In such cases, in fact, small disturbances from the real-time hip angle measurements can generate false orbits on the phase portrait, resulting in spurious signals for the phase variable $\phi(t)$, and the orbit will drive near the origin. The linear velocity is close to zero, and its estimate will drop as well. Thus, a start and stop walking detection algorithm is implemented to handle these events, where the real-time estimation of the subject's gait speed is compared to a predefined circular boundary centered around the phase portrait origin.

A stop event is detected when the phase portrait falls within the small predefined circular boundary. With reference to Figure 2.7, a radius equal to 70 is chosen as threshold; if the value is too large, slow walking pattern can be interpreted as stop events, whereas if the value is too small some occurrences may be missed because the normalization of the hip angle and angular velocity does not bring these variables exactly to zero, therefore the phase variable will not drop enough to lie in the small orbit. To prevent such cases, the phase should stay inside the boundary for at least 0.50 seconds to detect a real stop event. For the same reason, the restart is detected when both $r > 70$ and $|hipangle| > 15^{\circ}$ to make sure that the subject is approaching to a step: when the subject stops, he/she is supposed to stand in vertical position with an almost null hip angle. The hip angle condition is the same used in the detection of the first step when the person starts walking; basically, the period between the beginning of the trial and the first step is treated as a stop event.

The motor must follow and assist start and stop events. As anticipated, a stop event is treated like the interval before the detection of the first step, therefore the motor must go in default position: the system finds the closest default position (90 + offset, with the offset that now depends on the real-time value of the SGP) and the motor rotates accordingly. The transition from the actual position of the motor to the default position is not immediate but takes 0.12 seconds. As soon as the subject moves from a stop condition, the motor behaves exactly at the beginning of the trial, with a tailored profile of assistance for the first 2 or 3 steps.

The start and stop detection function will not be used for the experimental trials, but will be implemented and improved in the on-board version of the exosuit.

2.3 Software: Low-Level Control

The reference motion is the desired position of the motor. The device, however, is not directly driven with a position input, but rather with a velocity input, so the motor works in velocity mode. This choice is due to the hardware components adopted in our control system: since no force sensors are included, it is not possible to obtain representative information about the torque of the motor and to derive a meaningful motor reference torque command, which would require a deep knowledge of the features of the device in relation to the different characteristics of the person, therefore we preferred to have a control strategy which is independent of the anthropometry of the subject. To deal with a closed-loop system and provide a velocity command, a PID controller has been used. It takes the position error - the difference between the reference motion of the high-level control section and the current actual position of the motor recorded by the internal encoder - and converts it to the proper velocity for the motor. The PID has been manually tuned and the resulting filter has the following transfer function:

$$T(s) = k_p + k_i/s + k_d \frac{Ns}{s+N} \tag{2.15}$$

where $k_p = 25\, s^{-1}$, $k_i = 3\, s^{-2}$ and $k_d = 3$, with a filter coefficient N equal to 2.

2.3.1 Calibration

When the subject is ready to walk, the motor must lie in the default position as previously explained. However, before that, the device is in a "random" position which does not necessarily correspond to the intermediate point of the linear guide. Hence, it is necessary to run an automatic calibration procedure before each trial to drive the motor in the desired location.

The calibration requires both the rotary encoder on the external gear and the linear encoder of the guide. Any time the mechanism gets powered, the external encoder resets its measure and starts from zero. As the motor is turned on, it performs a 2.1π (378°) rotation at 2 rad/s which allows to detect the minimum and maximum linear guide positions with the corresponding motor positions. The intermediate point is found as the average between the two previous values, but there are two motor positions which correspond to the intermediate linear points: one in the range [0°-180°] and one in the range [180°-360°]. Following our convention, only the one that lies in the range [0°-180°] is correct and can be distinguished from the other by observing the occurrences of the maximum and minimum positions during the previous revolution. Accordingly, the motor slowly rotates towards such position following the shortest path. At this point, however, the rotary encoder can either display 90° or 450°: such value can be now used as an offset (initial encoder motor position) to make the reference motion match to the actual motion, which is essential for the PID controller. This last position is the desired default position. All the future readings of the motor position will be presented as:

$$actual\, MP = current\, encoder\, MP - initial\, encoder\, MP + 90$$

where MP stands for motor position.

During the calibration the algorithm creates a velocity command that drives the motor. This means that the device still works in velocity mode but in open-loop: the PID is not involved. When the calibration procedure terminates, a flag triggers the activation of the whole high-level control block and, few samples later, of the PID controller, in order to get a meaningful reference motion as input.

Chapter 3

Experimental Trials

At this point of the project it is necessary to test the goodness of the controller in relation to the characteristics of the mechanism. The behavior of the motor has been investigated from multiple point of views, with three main purposes:

- determine if the device is able to follow the movement of the leg during both locomotion modes, without discontinuities when switching between *alternation* and *alternation* to or any unexpected outcomes in the signal;
- quantify the accuracy of the two algorithms to discriminate between walking and running, also focusing on the transition phases and on the potential delay;
- extract relevant information in order to create a better profile of assistance, in terms of timing and of amount of cable to provide to the user

3.1 Methods

Following the previous guidelines, three tasks have been conducted on a treadmill:

- Walking task: subjects walked at 3, 5 and 7 km/h, each speed was maintaned for 75s;
- Running task: subjects run at 7, 9 and 11 km/h, each speed was maintaned for 75s;

- Mixed task: each speed was maintaned for 75s
  - 3 km/h Walking;
  - 7 km/h Running;
  - 7 km/h Walking;
  - 11 km/h Running;
  - 5 km/h Walking;

The single walking and running tasks are specifically related to the acquisition of features and all kinematic details for a better comprehension of the device-user interaction, whereas the combined task is more focused on the detection of the current locomotion mode and on the behavior during transition events. Consequently, the data coming from the first two tasks are windowed in intervals of 60s to address each speed separately, discarding the switch between activities, while the last task is fully analyzed also in the transition stages. Each trial was preceded by 30s of initial routine, which includes the starting of the acquisition, the check of the communication and the calibration procedure to start exactly at the default position of the motor. Two switches are employed to launch the procedure: one enables the communication first to check if all sensors are actually connected, then the other switch turns the motor on.

The duration of the trial is appropriate to acquire a sufficient number of steps at each velocity to make the analysis relevant. In the preliminary experiments the lowest cadence measured was about 0.75 Hz (45 steps/min), hence at least 20 steps per leg are taken when using windows of 60s.

Eleven healthy subjects participated to the test. Their demographic information are collected in Table 3.1. They all wore appropriate clothes for running. The focus is on the response of the hardware according to the movements of subjects as real-time inputs to the controller. As a consequence, no direct assistance is provided and subjects were equipped with a less complex structure: a belt carries one IMU on the back, while the other IMUs are tied to the thighs and are connected to the belt through a band to hold them in place and avoid their slide. Between the tasks they could rest for about 10 minutes, even if none of them needed more than few minutes given that they did not reach strenuous running speeds and due to the short duration of the trial. In addition, fatigue was not a relevant factor for this analysis and we could conduct the trials always in the same order.

Information	mean ± std	range
Age (yrs)	27.00 ± 1.90	[25 30]
Height (m)	1.78 ± 0.092	[1.63 1.93]
Leg Length (m)	0.94 ± 0.05	[0.86 1.02]

Table 3.1: Age and physical characteristics of the participants (n = 11)

As described in the hardware section, the entire control scheme runs on the Arduino MKR WiFi 1010 but the visualization and recording of data require the serial communication between the microcontroller and the PC, implemented on Simulink. Only the signals from the sensors are directly acquired (hip angle, hip speed, vertical acceleration of the IMU on the back, actual motor position, position of the linear guide); starting from them, a successive simulation is launched to acquire all the other meaningful feature for the analysis.

Walking and running share the same profile of assistance during this test: such strategy allows to evaluate the potential effectiveness of the timing of the cycle of assistance, looking for differences between the two modalities but also across multiple speeds. The worm gear mechanism has been set to produce a linear stroke of about 70mm.

The statistical significance analysis consisted in the preliminary check for Gaussian distribution of the data using the Kolmogorov-Smirnov test and then, stated that all data were not normally distributed, in the evaluation of the significant difference of the compared populations using the Wilcoxon runk sum test ($p < 0.05$).

3.2 Results

3.2.1 Correspondence between gait cycle and motor behavior

The main analysis is made to quantify the consistency of the motor behavior according to the user's motion. Figure 3.1 presents the trend of the position of the linear guide in function of the hip angle across different velocities. The coherence in frequency of the two signals reports values of 0.999, 0.999, 0.999 for the three walking speeds and 0.974, 0.996 and 0.995 for the three running speeds.

Figure 3.2 presents the occurrences of gait events for different speeds, whose

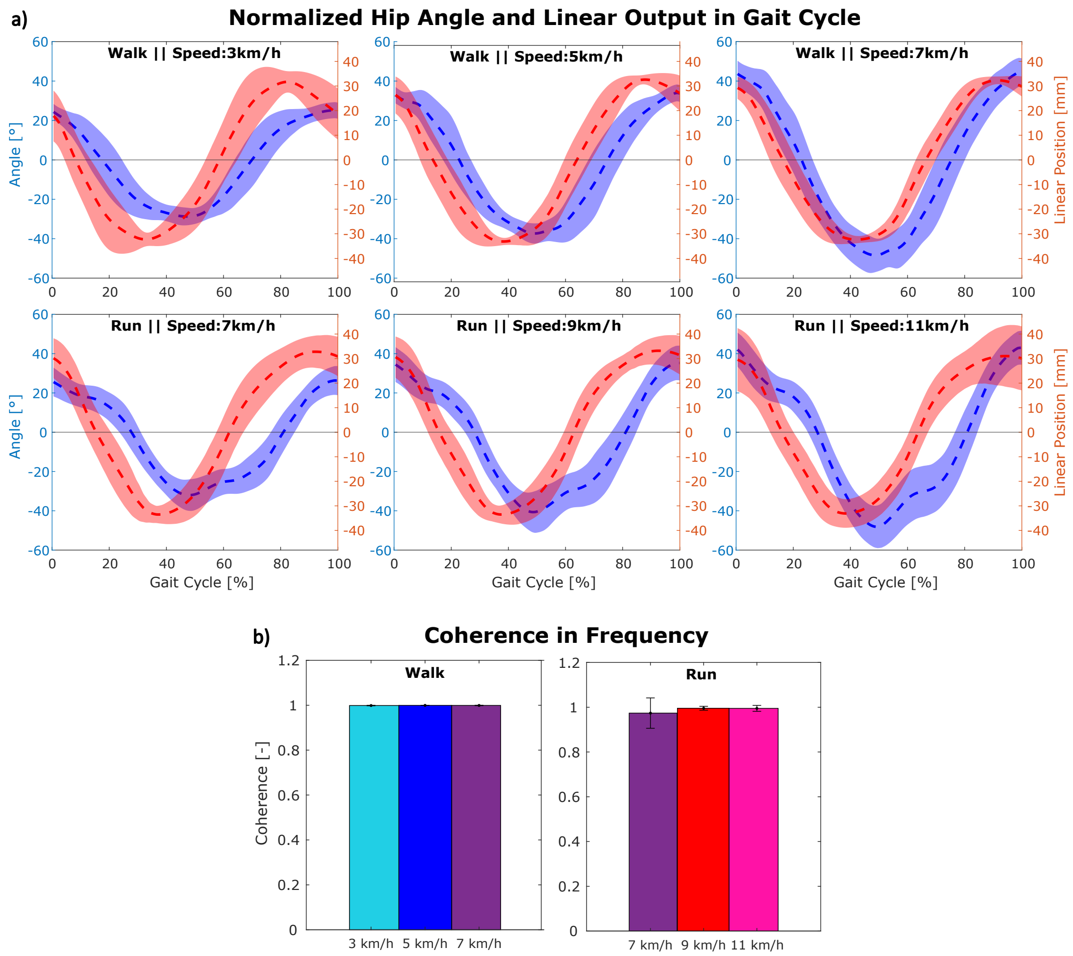

Figure 3.1: a) Trend of hip angle (blue) and position of the linear guide (red) as percentage of the gait cycle (between two successive step detection events with the right foot). The trends are averaged across the subjects. The dotted line represents the mean value, whereas the shaded portion is the area confined between mean $\pm$ standard deviation of data. b) Coherence between fundamental frequencies of hip angle and linear guide motion

average results are also reported in Table 3.2. The feature *Max Linear Output* actually refers to the starting point of the assistance instead of the peak of the signal: the event is detected when the position of the linear guide is 1mm less than the corresponding peak in module, which ensures a reliable value when the guide is almost stationary at the extremity of the device.

The different evolution of the motor position in the gait cycle depending on the locomotion mode is presented in Figure 3.3. In *alternation* motion the motor shifts from an average minimum position of 13.17° to an average

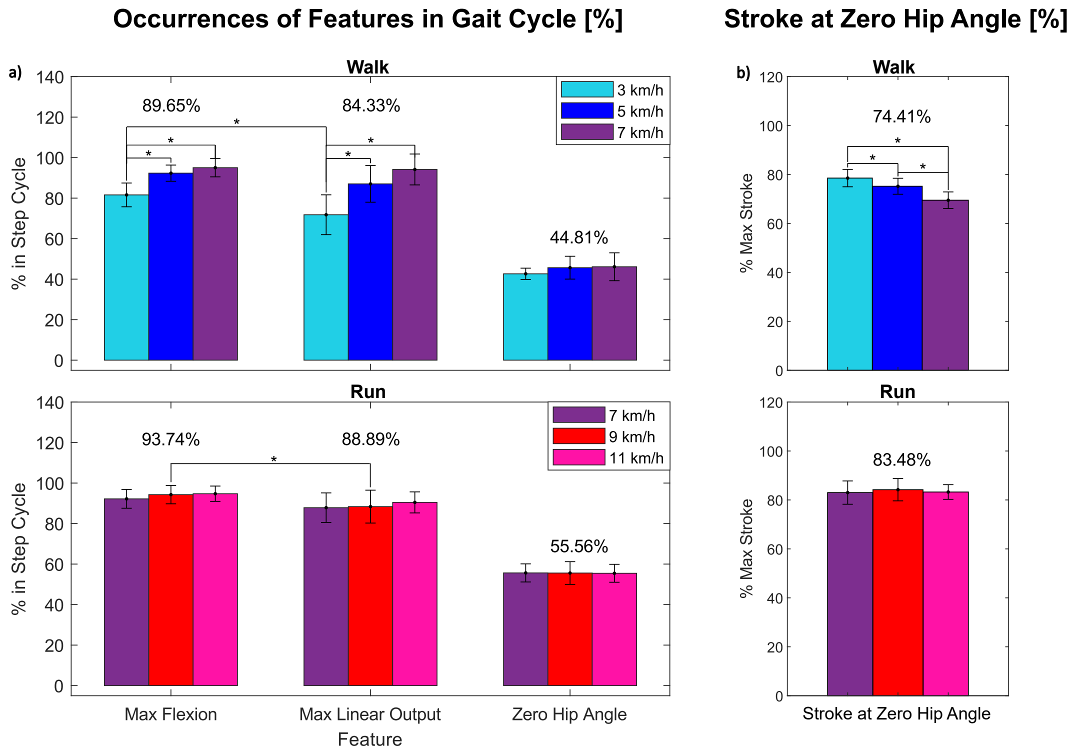

Figure 3.2: Occurrences of events in step cycle across different speeds for walk (top) and run (bottom). The average occurrence of an event is reported above each group. b) Actual linear stroke at the moment of zero hip angle in percentage of the entire excursion.

		Event			
Mode	Speed	Flex	LinOut	ZHA	Stroke at ZHA
Walk	3	81.59 ± 5.86	71.80 ± 9.84	42.64 ± 2.78	78.54 ± 3.55
	5	92.32 ± 4.00	87.03 ± 9.05	45.66 ± 5.64	75.19 ± 3.27
	7	95.04 ± 4.52	94.16 ± 7.63	46.12 ± 6.89	69.49 ± 3.39
Run	7	92.21 ± 4.65	87.84 ± 7.31	55.64 ± 4.47	83.00 ± 4.77
	9	94.28 ± 4.52	88.37 ± 8.12	55.58 ± 5.61	84.19 ± 4.56
	11	94.74 ± 3.78	90.46 ± 5.19	55.45 ± 4.42	83.24 ± 3.00

Table 3.2: Average occurrences of gait events. Values reported as mean ± standard deviation, in percentage. Label of events: Flex = Max Flexion; LinPos = Max Linear Output; ZHA = Zero Hip Angle. Speeds are in km/h

maximum position of 157.49°, while in *rotation* motion the motor is around 21.79° at the beginning of the gait cycle and at 376.26° (16.26° of the following revolution) at the end. The average delay of the actual motion with respect to the reference one is 0.106s.

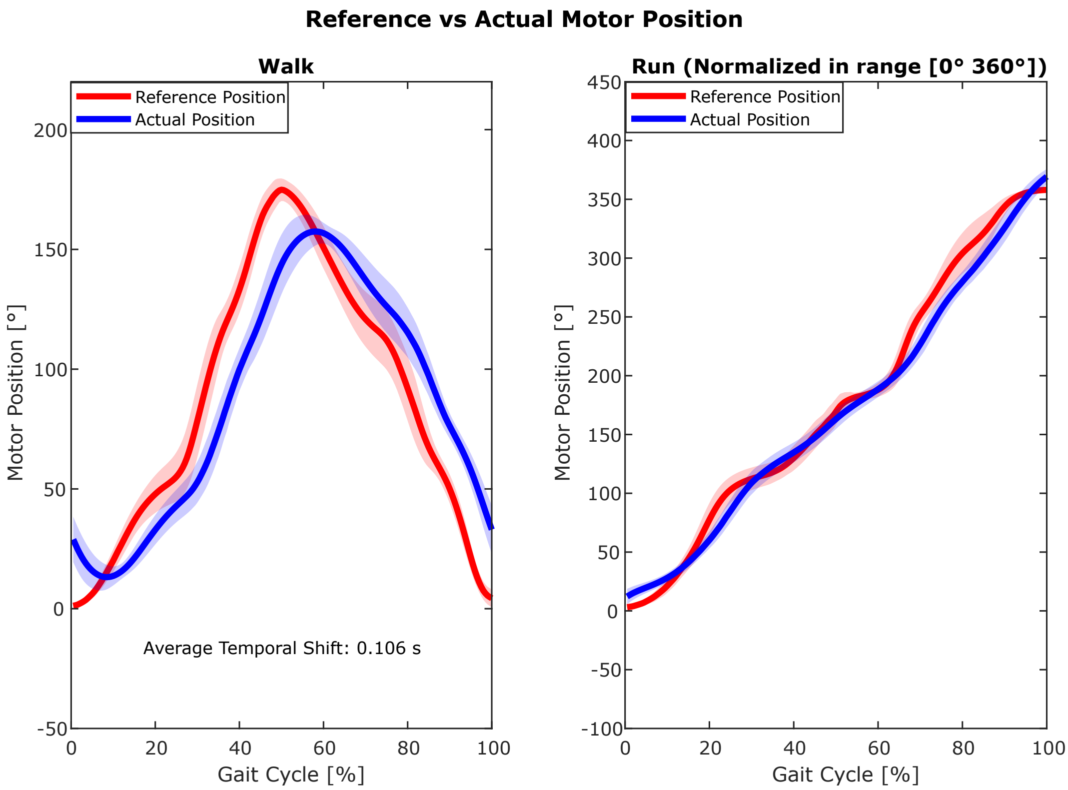

Figure 3.3: Comparison between reference (red) and actual (blue) motor position during walking and running. Data are relative to one subject.

3.2.2 Accuracy of the methods for discern walking and running

The average value of the vertical acceleration during each section of the trial, reported in Figure 3.4, is (0.409, -7.754, 2.971; -5.944; 4.863) $[m/s^2]$. The mixed trial reported a total accuracy of 98.52% for the 3-IMU method and an accuracy of 92.51% for the 2-IMU method. Figure 3.5. The quantification of the delay of the detection using the two algorithms in collected in Table 3.3

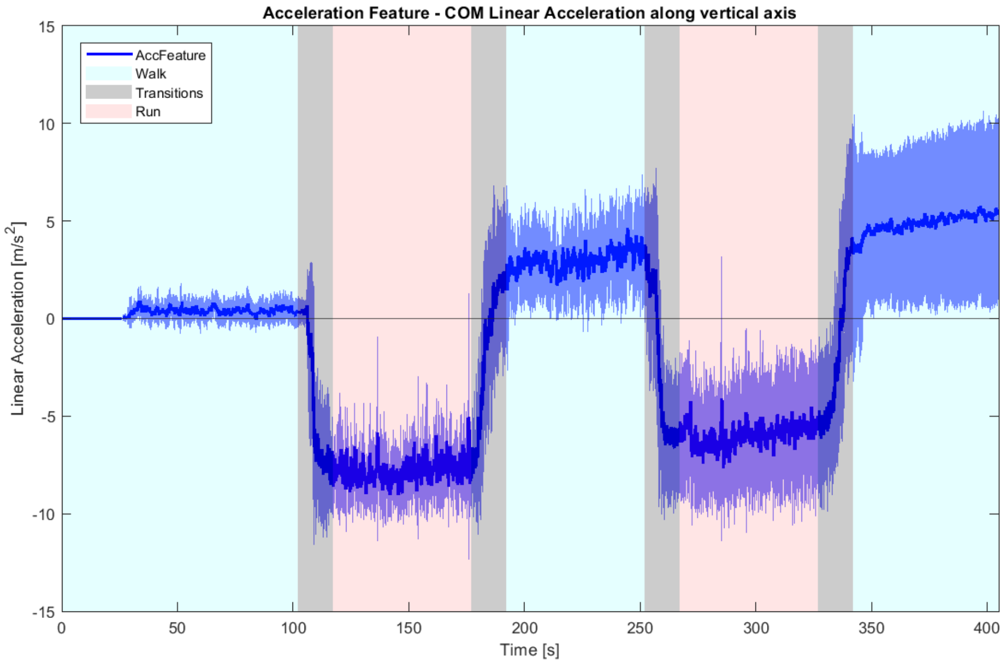

Figure 3.4: Trend of the acceleration feature for the walk/run discrimination across the mixed task. It is expressed as average value (main line) ± the standard deviation (shaded area) at each instant

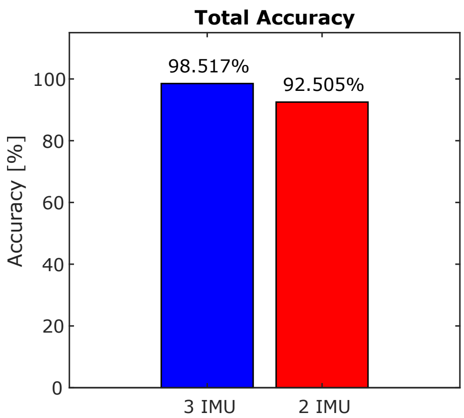

Figure 3.5: Accuracy of the 2-IMU and 3-IMU methods in detecting walking and running during the mixed trial

Subject	Number of steps			
	W → R (T1)	R → W (T2)	W → R (T3)	R → W (T4)
1	21	23	23	5
2	1	0	2	-18
3	2	-2	1	-3
4	2	-1	-7	0
5	5	1	2	13
6	3	0	1	4
7	2	1	1	4
8	2	-13	3	-19
9	2	2	-1	1
10	0	-1	1	0
11	1	-8	2	6
Mean ± SD	3.7 ± 5.9	0.2 ± 8.8	2.5 ± 7.3	-0.6 ± 9.8

Table 3.3: Distance (in terms of number of steps) in the detection of the transition between the two methods. A positive value x means that the detection with the 3-IMU method occurred x step before the one with the 2-IMU method.

3.2.3 Additional characteristics of the device

Figure 3.6 describes how the motor actually rotates in alternation motion as the human cadence increases. The equations of both regression lines are written in Figure 3.6.a). Figure 3.6.b) shows only the trend of the linear guide position, since it is more indicative of the motor behavior in such conditions. The specific data for the histogram are reported in Table 3.4. Finally, the average hip angle peak for each subject across the trials is reported in Figure 3.7 and in Table 3.5

Range (steps/s)	1.00 → 1.25	1.25 → 1.50	1.50 → 1.75
Values (%)	99.24 ± 0.51	99.00 ± 0.98	97.40 ± 1.50
Range (steps/s)	1.75 → 2.00	2.00 → 2.25	2.25 → 2.50
Values (%)	96.31 ± 1.81	94.57 ± 2.08	92.21 ± 1.47

Table 3.4: Average percentage of actual stroke with respect to the maximum one. Range are in steps/s, while values are reported as mean ± standard deviation

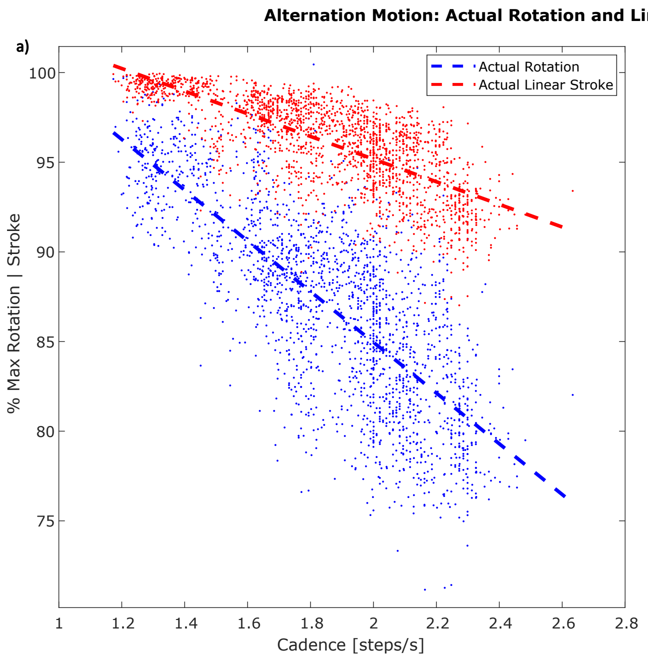

Figure 3.6: a) Actual rotation (blue) of the motor and actual linear stroke (red) in function of cadence in *alternation* motion condition. All data points are expressed in percentage of the maximum stroke for the corresponding trial and refer to a complete cycle of assistance (0° → 180° → 0°); the dashed line describes the trend of points according to the least square method. b) Trend of actual linear stroke in function of cadence - Histogram. Samples are collected in ranges of 0.25 steps/s.

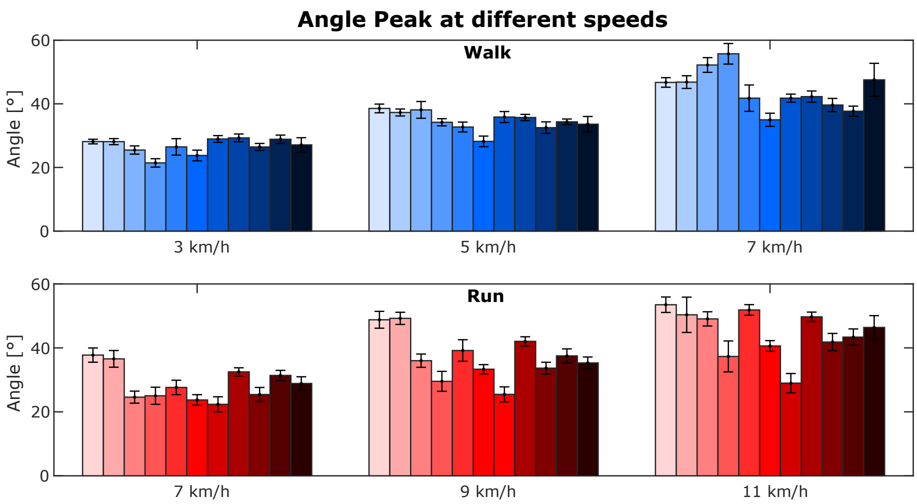

Figure 3.7: Average angle peaks for each subject at different speeds. The subjects are sorted in ascending order according to their height.

Subject	Height [m]	Angle Peak [°]					
		W at 3	W at 5	W at 7	R at 7	R at 9	R at 11
1	1.63	28.14	38.55	46.73	37.75	48.79	53.50
2	1.65	28.12	37.28	46.84	36.57	49.24	50.35
3	1.68	25.48	38.10	52.21	24.60	36.00	49.07
4	1.73	21.44	34.20	55.73	25.03	29.54	37.33
5	1.80	26.47	32.71	41.78	27.63	39.18	51.87
6	1.80	23.77	28.20	34.98	23.72	33.33	40.61
7	1.80	28.95	35.85	41.79	22.36	25.47	28.98
8	1.83	29.30	35.70	42.27	32.51	42.04	49.72
9	1.83	26.45	32.51	39.63	25.42	33.67	41.83
10	1.85	28.87	34.35	37.68	31.39	37.50	43.37
11	1.93	27.11	33.59	47.54	28.87	35.30	46.39

Table 3.5: Average angle peaks [°] at each speed for each subject

Chapter 4

Evolution of the project

4.1 Discussion of results

4.1.1 Correspondence between gait cycle and motor behavior

From a very first look at the outcomes, the primary purpose of driving the motor according to the subject's motion has been properly reached. The trend of the linear guide position and the hip angle (Figure 3.1) are always concordant, both with an overall low standard deviation. On one side, this highlights the similar walking (and running) pattern of all the participants, on the other the motor moves with the right timing during the entire trial, at different speeds. The standard deviation of the linear position is slightly higher in correspondence to the end/beginning of the gait cycle while running at 11 km/h, due to the fact that this is the point around which the assistance starts and a tiny difference in the hip angle between subjects or even between steps of a single participant may induce a minimal variation of the starting time of the guide, which is nevertheless irrelevant for the correct functioning. This is less pronounced in all the other conditions, but it seems to happen only at the detection of the right step (around 0% or 100%) and not when at the detection of the left step (around 50%): this fact may suggest to investigate also the symmetry between left and right step in terms of motor outcomes to understand if it can be explained with a physiological asymmetrical trend of the gait of the subject or it is due to a different performance of the algorithm in the detection of the step from both legs.

A further evidence of the ability of the motor to follow the human motion is given by the coherence: the analysis has been made just for the fundamental frequency of each signal (which is supposed to be the average cadence during the entire section of the trial) and all values are very high without statistical difference between speeds.

The quantitative analysis of the timing of the gait features and motor events inside a step cycle (Figure 3.2) reports that there is a significant difference between the timing of the maximum flexion of the leg and the beginning of the cycle of assistance for the 3 km/h walking and for the 9 km/h running task, with the linear motion that anticipates the occurrence of the maximum flexion. Considering that the two events must be almost simultaneous, and looking also at the other pair of values, the result suggest to postpone the beginning profile of assistance of few samples. No difference comes out from the further comparisons of features in the same section. On the other side, the percentage of overall occurrence of the maximum flexion is delayed with respect to the value obtained in the preliminary study (Figure 2.16), which may indicate that the starting point of profile of assistance should instead be anticipated to match the desired hip torque portrait. This counterindicative pieces of information lead to the conclusion that to find the proper timing for the beginning of the assistance it is necessary to ask the users' sensation while wearing the exosuit and actively receiving support from the motor.

Focusing on the final part of the cycle of assistance, the occurrence of the zero hip angle of both walking and running are concordant to those of the preliminary results. In walking, the rising trend of the occurrence of the zero hip angle as the subject accelerates, associated to the falling trend of the percentage of completed stroke at that specific instant (with statistical difference between speeds), suggests that the profile of assistance should be modeled in function of the gait speed and progressively delay the end when the user walks faster. In running, the timing of zero hip angle and the actual stroke at that moment are stationary and independent of the speed. The zero hip angle occurs later in the gait cycle in running than in walking and also the actual excursion is larger. Responses from the participants will be useful to tell if the end profile of assistance must be anticipated or delayed, which means to obtain a higher or lower percentage of actual stroke at the moment of zero hip angle, respectively.

An additional observation is made on the diversities in the features across the speeds: the maximum flexion and the starting point of the assistive profile during walking at 3 km/h happen statistically earlier with respect to faster walking, whereas in running the speed does not affect the timing of occurrence of the features.

The comparison of the reference position command and the actual motor position in Figure 3.3 reveals that the actual position is delayed of about 0.1 seconds in *alternation* mode. This is partly due to the delay introduced by the algorithm, especially in the process of normalization of the hip angle and angular velocity or in the use of the Kalman filter, and partly to the intrinsic delay of the communication between the sensors and the control unit. Even if the step time can decrease significantly when the cadence is high, such delay is admissible in this kind of applications because it can be compensated by tuning the assistance properly. In *rotation* mode the actual position does not precisely follow the reference command but still acceptable: it is a trade-off between responsiveness and smooth motion. The actual position is above the reference one at the boundaries of the gait cycle, exceeding the 360° limit, while the two intersect multiple times in the middle of the gait cycle.

4.1.2 Accuracy of the methods for discern walking and running

The ability to distinguish walking from running is a crucial part of the system. The preliminary test showed that the 3-IMU method had a better overall accuracy in the detection, as expected, and it has been chosen for the experiments to mark the transition between *alternation* and *rotation* mode. The final trials reported that the 3-IMU method is still the most accurate (98.52%, even better than the previous test) but also the 2-IMU method performed better (92.51% against 87.81%). These results are very promising; nevertheless it is worth to underline few aspects.

As presented in Figure 3.4, the mean of the acceleration in correspondence to the maximum extension of the hip is totally different for the two activities and that enables a relatively straightforward discrimination. However, the average value in walking is really close to zero and sometimes it display fluctuations that cross the zero line. This is not an issue when the subject preserves the walking gait because the threshold of $-1.5 m/s^2$ prevents from the incorrect detection of the running activity and two consecutive steps with negative feature are necessary to enable the transition (unless the feature is greatly negative). But when the person changes from running to walking, the switch occurs when the feature is higher than $+1.5 m/s^2$ and still positive afterwards; being the acceleration close to zero, this transition may be quite slow. On the other side, the feature during running is usually distant from the threshold line, therefore a wrong response of the system is highly improbable. Furthermore, this profile often allows to obtain a fast single-step transition between walking to running because the value is below $-5m/s^2$.

This becomes evident when looking at the outcomes of Table 3.3. The table presents the delays as difference of number of steps needed by the two algorithms to detect a change in the gait mode: the real transition usually requires few steps, hence it is not possible to identify a specific time instant. The walk-to-run transitions are almost always detected earlier by the 3-IMU method: as previously explained, the transition is usually fast because of the huge drop of the acceleration features. The 2-IMU method is still quite fast, but it does not allow a single-step transition: it requires two steps to enable it. On the other hand, the mean value of the delays for the run-to-walk transitions are around zero: this means that one algorithm can perform better than the other just depending on the situation. For instance, when the 2-IMU method detects the transition much faster than the 3-IMU one (highly negative number in the table), it is an indication that the acceleration feature has not become enough positive to exceed the $+1.5m/s^2$ threshold and the the transition will take much more time. On the other hand, a significantly delayed detection of the 2-IMU method with respect to the other can suggest that the model for the corresponding subject is not appropriate for the discrimination between locomotion modes.

In addition, the feature of the acceleration during the mixed trial usually has a rising trend: the acceleration measure is affected by drift, as it happens for the angle. The standard deviation of the signal increases as time flows: the detection of the locomotion mode has barely been affected by the drift because of the limited duration of the trial, but it must be eliminated to ensure a reliable detection even in prolonged activities. An unexpected behavior is that the drift always drives the signal upwards, when present: we would expect a random direction of the drift and not a systematic phenomenon, therefore a deeper analysis will be necessary.

The 3-IMU method has the huge advantage of reaching a very high accuracy without the use of data-driven methods (Machine Learning for instance). This means that the controller does not need pre-training or computational intensive resources and it is still able to generalize the "classification" being independent of the anthropometry of the subjects. The 2-IMU method, instead, requires a preliminary creation of the model and is based on a default error in the estimation of the speed during running, therefore it is intrinsically inaccurate. Moreover, having a single model for multiple subjects of the same height is not doable because they may show distinct gait patterns and reach different angle peaks. Nevertheless, the 2-IMU approach may really become a interesting option in the next years if the technology enables a more reliable reading of the angle measure because the reduction of the number of sensors would be helpful to prevent communication issues.

4.1.3 Additional characteristics of the device

In this version of the control system, the distinction between walking and running is essential to drive the motor and the actual motor modality exclusively depends on the detection of the current locomotion modes. However, this innovative mechanism has been realized with the main intent to avoid all the issues related to the inversion of the direction of rotation of the motor. The detection of the correct locomotion mode helps solve this problem because walking and running are usually associated to low and high speed respectively, but since the motor reverses its direction any time a leg is at full flexion, the parameter of interest is neither the locomotion mode nor the speed, but rather the cadence. The cadence directly indicates how often the motor should rotate the direction of rotation if the $alternation$ mode is preserved; on the other side, the detection of walking and running (or the speed) can just suggest what the correct behavior of the motor should be.

Running usually involves high cadences also at very low running speed (jogging) because the person jumps and bounces to the ground, according to the "leg spring" model, hence it is reasonable to always drive the motor in $rotation$ mode when running is detected. In walking, instead, the cadence can be more or less high depending on the speed and on the characteristics of the person. Considering the characteristics of the device, it may be convenient to switch to the spinning mode when the cadence exceeds a fixed limit. The histogram in Figure 3.6.b), where the actual excursions are collected in groups of 0.25 steps/s, shows that in $alternation$ mode, the actual stroke is reduced significantly even when the cadence falls in the range [1.50 1.75] steps/s, taking as reference the stroke associated to the lowest range (< 1.25 step/s). No statistical difference is present between the first and second range, while the difference progressively becomes larger when the cadence increases. Actually, the reduction of the excursion is minimal even at the highest cadence (92.21% of the maximum stroke during walking with a cadence > 2.25 steps/s, but the corresponding reduction of the motor is relevant (around 80% from Figure 3.6.a)), therefore a good option would be to take both the actual locomotion mode and the cadence into account to define the working modality of the motor.

Figure 3.7 finally displays the average angle peaks for each subject at each velocity, reflecting that there is no link between the range of motion of the person and the height. This has implication on the future considerations about the cable length needed by the person to effectively receive support: given the locomotion mode and the travelling speed, the height cannot be used to derive the right amount of cable because the fluctuations in the graph are very large.

4.2 Future Development

The current version of the control system was specifically thought for an off-board system to be tested in a standardized environment, on a treadmill. The results confirmed the ability of the motor to follow the gait pattern of the user, therefore the very next step involves the use of the real exosuit to verify if the device fits the goal to provide the desired assistance. To do that, a check of the structure must take place. The robustness of the device must be checked to avoid high torques in some edges or corners in the structure and more resistant to bear the loads that are required for the proper assistance. On the other side, a compliant element must be introduced to dissipate the tension transferred to the mechanism and to preserve the robustness of the structure. Hence, an important decision will be whether to keep the compliant rings in the tendons or put a new component on the mechanical design (or both).

Once the off-board version of the device works, the on-board one must be realized. It will require few modifications of the main mechanism: the structure must be lightened, the motor must be placed in a proper location and the control unit and all the wires must be collected in a case that should be as compact and comfortable as possible. The communication strategy will be an important step: the fact that the entire control system runs on just the Arduino MKR Wifi 1010 is definitely the best option for its simplicity and because it avoids the need to implement a data transfer between multiple microcontrollers, an operation that always slows down the processing of the algorithm. However, the employment of many sensors like the two external encoders, in addition to the three IMUs, makes the stream of data not easy to handle and reduces the margin of improvement of the control unit in terms of new functionalities of the system, since the microcontroller will be overloaded. As it stands, for the same reasons, we have limitations in the number of signals to send to the PC for visualization. Therefore, we might consider to split the burden of the algorithm between more microcontrollers and find the best way to combine them for the acquisition of the signals from the sources, the creation of the reference command and the execution of the low-level control. This is essential until the development process goes on, during which the more information we manage to collect about the device, the faster we can improve the system: at the very end, the two external sensors and the visualization of signal will no longer be needed and the communication will be relieved.

Concerning the control part, the whole scheme will be preserved in the future version of the project, given the promising outcomes of the tests. The main focus will be put on the tuning of the profile of assistance: as previously said, the creation of an effective trajectory requires a long trial-and-error process where the feelings of the user are the best information, both in terms of timing and of entity of the support. The starting and ending point of the profile have already been discussed: the anticipation or the postponement of these two events is the result of a combination between the introduction of a corrective factor in the creation of the gait phase, which simply shifts the sinusoidal gait phase signal in time, and the appropriate tuning that widens or shrinks the interval of actual assistance.

The entity of the support is instead associated to the amount of cable provided to the person and, therefore, to the actual stroke of the linear guide. The quantification of cable is essential and there is a tiny margin of error: if the excursion is too large, the cable will be slack at the beginning of the cycle with no assistance provided at the starting of the linear guide movement, while at the middle of the cycle the action of the motor will be too strong; on the other hand, a very small stroke restricts the range of motion of the user that would otherwise pull the motor against its physical limitations. Moreover, the subject must be free to accelerate or decelerate, to switch from walk to run or vice-versa, hence the range of motion will change during the gait and the length of cable must be modified accordingly to avoid the aforementioned issues. Therefore, in the next prototype, the secondary motor will have an active role in the mechanism and it will be driven by the control unit to adaptively change the cable length in function of the user's speed and range of motion.

However, the last analysis shows that the range of motion evaluated at the same speed is neither constant nor a function of the height, but is different from subject to subject, hence the correct length is difficult to obtain. One possible approach consists in conducting preliminary trials on the user to see how the range of motion and the consequent cable length vary at different speeds, in order to create a model. It would require an initial condition: the idea is to measure the distance between the belt anchor point and the thigh anchor point in vertical position and at a specific range of motion or angle of the leg in flexion (30° degrees). Considering that the extension consists of 15° degrees at most and that the profile of assistance should terminate in correspondence to the zero hip angle, we can conclude that the difference in the distances is approximately the amount of cable needed to just follow the movement of the subject. Then, this length should be increased by a factor to obtain an effective action of the device on the user. The other approach relies on the creation of a priori model based only on the subject's height: under the assumptions that the leg length is always proportional to the height and that the belt and thigh wraps are always put at the proper anatomical positions, the amount of cable needed by the subject to span a fixed range of motion is a linear function of the height (taller subjects need more cable to have the same range of motion). After tuning this length at a standard angle, the control scheme will gradually modify the maximum excursion of the linear guide in function, for instance, of the latest angle peaks.

Independently of the approach, there are two intrinsic limitations. The hip exosuit is underactuated, so it coordinates both legs with a single motor; however, since the extension of one leg is not perfectly simultaneous to the flexion of other, there will be short phases during the gait cycle where one leg goes against the movement of the motor, in particular at the beginning/end of the cycle of assistance. If the profile is correctly tuned, this is a negligible issue. The other is related to the settings of the cable length at the initial moment of the trial. Before starting, the person is in standing position with almost completely tight cable, and as soon as the intention of the first step is detected the motor moves accordingly. However, considering that the subject can move whatever leg to start the motion, a sufficient amount of cable will be necessary in both directions of the linear guide. This means that an overall larger amount of cable is provided to the user, which implicates the already discussed drawbacks. These limitation require specific attention and enhance the need for an optimal profile of assistance.

Furthermore, different profiles of assistance will be used separately for walking and running. While the current strategy may be fine for walking and just requires the correct tuning, running is a more vigorous activity a specifically needs a huge support in the propulsive phase. Therefore, an impulsive profile of assistance just before the HS of the forward leg could be an interesting option.

After a general optimization of the algorithm, considerations about the current approach to compensate the drift of the angle will be made: it has the advantage of using just 2 signals from each IMU but works well only in straight direction, because any wrong peak detection during turnings may threaten the correct development of the signal. The secondary motor must be fast to adapt to the real-time range of motion, and the functionality to detect stop events and move the motor consistently will be added. Finally, higher running speeds will be hopefully investigated to test both the ability of the device to work at even larger cadences and to tell whether the hypothesized strategies to determine the right amount of cable are still valid.

Chapter 5

Conclusion

The design of an exosuit for running assistance has the purpose to broaden the range of lower-limb movements that a person can perform. Starting from walking, the most fundamental kind of human motion, more activities have progressively been addressed, from tasks of daily living such as sit-to-stand or climb and descend stairs to more vigorous activities like running. Great attention and effort is currently put on running: there is the desire to move out from a standardized environment, to support a more complex and rapidly-varying movement and to reduce people's muscular effort also during training or sport. So far, few devices have been realized to enhance running performance. Despite obtaining promising results, they all present a main limitation: the difficulty in reversing the motor direction of rotation to assist one leg after the other, because of the motor inertia. This issue comes out especially at higher cadences, leading to the impossibility to drive the motor correctly at high running speeds and therefore being unable to provide the best profile of assistance.

Our innovative design overcomes the previous limitation: it is based on a Cardan Gear mechanism that allows the motor to spin continuously so that it does not work against its own inertia and broadens the bandwidth of the system to easily withstand the higher step frequency during running. The mechanism converts the continuous rotation of the motor to a linear, confined movement of a guide that travels from side to side of the device to provide support during each leg's extension and represents the direct action of the mechanism on the user, by alternately retrieving and releasing the cable. The features of the device allow to modulate the amount of cable to provide to the person according to his/her height and current locomotion mode by simply rotating a gear on the top of the mechanism, a procedure that can be done either before the trial or even in real-time when the person wants to change speed or switches from walk to run or vice-versa.

The other great feature of the system is the ability to detect the current locomotion mode in real-time. Walking and running present dissimilar energy profiles and gait patterns, so their identification allows to drive the motor properly in each condition. Two methods for discrimination have been developed, based on totally different kinematic principles. These algorithms are included in a control scheme that derives all the relevant temporal and spatial gait parameters starting from just 5 kinematic signals acquired from 3 IMU sensors, leading to a simple and lightweight structure.

Experiments have been conducted to investigate the overall robustness of the control unit, which reported the ability of the motor to follow the motion of the user at different speeds, both in walking and running. The accuracy in detecting the current locomotion mode has been great with both algorithms, revealing an hypothetical opportunity to reduce the number of sensors in the future for discrimination purposes, and the transitions between walking and running have been promptly detected with generally a maximum of few steps of delay.

The outcomes of the previous tests are really promising and push us to the continuous development of the exosuit, which initially requires a more solid structure to withstand the physiological loads of the human gait and involves the optimization of the algorithm and the proper tuning of the profile of assistance. After checking the stability of the communication and creating a compact and comfortable case for the hardware components, the final version of the exosuit will be completed and evaluated in all its characteristics, with the ultimate purpose to reduce the metabolic cost of the human walking and running.

This project wants to emphasize why soft exoskeletons are progressively getting much attention, underlining their potential application not only for traditional daily living activities but also for more energetic and complex tasks and actions like running. Despite this device was specifically intended for metabolic reduction purposes in running, it can also be adopted for walking assistance. Moreover, it would be interesting to merge the functionalities of different exosuits into a single system to address any possible need of the user. Hopefully, exosuits will be a common assistive device in people's lives in few decades from now, thanks to their portability, simplicity of use and reliability.

Bibliography

[1] S. Net'uková, M. Bejtic, C. Malá, *et al.*, "Lower limb exoskeleton sensors: State-of-the-art," *Sensors*, vol. 22, no. 23, p. 9091, 2022.

[2] H. T. T. Vu, D. Dong, H.-L. Cao, *et al.*, "A review of gait phase detection algorithms for lower limb prostheses," *Sensors*, vol. 20, no. 14, p. 3972, 2020.

[3] C. T. Farley and D. P. Ferris, "10 biomechanics of walking and running: Center of mass movements to muscle action," *Exercise and sport sciences reviews*, vol. 26, no. 1, pp. 253–286, 1998.

[4] K. F. Bowman Jr, J. Fox, and J. K. Sekiya, "A clinically relevant review of hip biomechanics," *Arthroscopy: The Journal of Arthroscopic & Related Surgery*, vol. 26, no. 8, pp. 1118–1129, 2010.

[5] B. Chen, B. Zi, L. Qin, and Q. Pan, "State-of-the-art research in robotic hip exoskeletons: A general review," *Journal of orthopaedic translation*, vol. 20, pp. 4–13, 2020.

[6] A. F. Pérez Vidal, J. Y. Rumbo Morales, G. Ortiz Torres, *et al.*, "Soft exoskeletons: Development, requirements, and challenges of the last decade," in *Actuators*, MDPI, vol. 10, 2021, p. 166.

[7] F. Eyüboğlu, Ç. Sayaca, M. Çalik, D. Korkem, L. N. Tascilar, and D. Kaya, "Kinesiology of the hip," in *Comparative Kinesiology of the Human Body*, Elsevier, 2020, pp. 375–392.

[8] Y. Dong, "Study and realization of the training control system of a rehabilitation exoskeleton orthosis for lower limbs," *Zhejiang University: Hangzhou, China*, 2008.

[9] X. Tang, X. Wang, X. Ji, *et al.*, "A wearable lower limb exoskeleton: Reducing the energy cost of human movement," *Micromachines*, vol. 13, no. 6, p. 900, 2022.

[10] P. Malcolm, W. Derave, S. Galle, and D. De Clercq, "A simple exoskeleton that assists plantarflexion can reduce the metabolic cost of human walking," *PloS one*, vol. 8, no. 2, e56137, 2013.

[11] G. S. Sawicki, O. N. Beck, I. Kang, and A. J. Young, "The exoskeleton expansion: Improving walking and running economy," *Journal of neuroengineering and rehabilitation*, vol. 17, no. 1, pp. 1–9, 2020.

[12] M. van Wijdeven, "Design and evaluation of a passive hip exoskeleton to reduce the energy cost of human walking," 2016.

[13] I. Kang, H. Hsu, and A. Young, "The effect of hip assistance levels on human energetic cost using robotic hip exoskeletons," *IEEE Robotics and Automation Letters*, vol. 4, no. 2, pp. 430–437, 2019.

[14] T. M. Miller-Jackson, R. F. Natividad, D. Y. L. Lim, L. Hernandez-Barraza, J. W. Ambrose, and R. C.-H. Yeow, "A wearable soft robotic exoskeleton for hip flexion rehabilitation," *Frontiers in Robotics and AI*, vol. 9, p. 835 237, 2022.

[15] T. Zhou, C. Xiong, J. Zhang, D. Hu, W. Chen, and X. Huang, "Reducing the metabolic energy of walking and running using an unpowered hip exoskeleton," *Journal of NeuroEngineering and Rehabilitation*, vol. 18, no. 1, pp. 1–15, 2021.

[16] R. C. Browning, J. R. Modica, R. Kram, and A. Goswami, "The effects of adding mass to the legs on the energetics and biomechanics of walking," *Medicine & Science in Sports & Exercise*, vol. 39, no. 3, pp. 515–525, 2007.

[17] A. T. Asbeck, K. Schmidt, and C. J. Walsh, "Soft exosuit for hip assistance," *Robotics and Autonomous Systems*, vol. 73, pp. 102–110, 2015.

[18] S. Jin, N. Iwamoto, K. Hashimoto, and M. Yamamoto, "Experimental evaluation of energy efficiency for a soft wearable robotic suit," *IEEE Transactions on Neural Systems and Rehabilitation Engineering*, vol. 25, no. 8, pp. 1192–1201, 2016.

[19] J. Kim, B. T. Quinlivan, L.-A. Deprey, *et al.*, "Reducing the energy cost of walking with low assistance levels through optimized hip flexion assistance from a soft exosuit," *Scientific reports*, vol. 12, no. 1, p. 11 004, 2022.

[20] E. Tricomi, N. Lotti, F. Missiroli, *et al.*, "Underactuated soft hip exosuit based on adaptive oscillators to assist human locomotion," *IEEE Robotics and Automation Letters*, vol. 7, no. 2, pp. 936–943, 2021.

[21] W. Cao, C. Chen, H. Hu, K. Fang, and X. Wu, "Effect of hip assistance modes on metabolic cost of walking with a soft exoskeleton," *IEEE Transactions on Automation Science and Engineering*, vol. 18, no. 2, pp. 426–436, 2020.

[22] L. Chen, C. Chen, X. Ye, *et al.*, "A portable waist-loaded soft exosuit for hip flexion assistance with running," *Micromachines*, vol. 13, no. 2, p. 157, 2022.

[23] J. Yang, J. Park, J. Kim, S. Park, and G. Lee, "Reducing the energy cost of running using a lightweight, low-profile elastic exosuit," *Journal of NeuroEngineering and Rehabilitation*, vol. 18, no. 1, p. 129, 2021.

[24] R. Nasiri, A. Ahmadi, and M. N. Ahmadabadi, "Reducing the energy cost of human running using an unpowered exoskeleton," *IEEE Transactions on Neural Systems and Rehabilitation Engineering*, vol. 26, no. 10, pp. 2026–2032, 2018.

[25] J. Kim, G. Lee, R. Heimgartner, *et al.*, "Reducing the metabolic rate of walking and running with a versatile, portable exosuit," *Science*, vol. 365, no. 6454, pp. 668–672, 2019.

[26] F. Missiroli, N. Lotti, E. Tricomi, *et al.*, "Rigid, soft, passive, and active: A hybrid occupational exoskeleton for bimanual multijoint assistance," *IEEE Robotics and Automation Letters*, vol. 7, no. 2, pp. 2557–2564, 2022.

[27] X. Zhang, E. Tricomi, F. Missiroli, *et al.*, "Enhancing gait assistance control robustness of a hip exosuit by means of machine learning," *IEEE Robotics and Automation Letters*, vol. 7, no. 3, pp. 7566–7573, 2022.

[28] E. Tricomi, M. Mossini, F. Missiroli, *et al.*, "Environment-based assistance modulation for a hip exosuit via computer vision," *IEEE Robotics and Automation Letters*, vol. 8, no. 5, pp. 2550–2557, 2023.

[29] D. Quintero, D. J. Lambert, D. J. Villarreal, and R. D. Gregg, "Real-time continuous gait phase and speed estimation from a single sensor," in *2017 IEEE Conference on Control Technology and Applications (CCTA)*, IEEE, 2017, pp. 847–852.

[30] J. Nilsson and A. Thorstensson, "Adaptability in frequency and amplitude of leg movements during human locomotion at different speeds," *Acta Physiologica Scandinavica*, vol. 129, no. 1, pp. 107–114, 1987.

[31] K. Seo, "Real-time estimation of walking speed and stride length using an imu embedded in a robotic hip exoskeleton," in *2023 IEEE International Conference on Robotics and Automation (ICRA)*, IEEE, 2023, pp. 12 665–12 671.

[32] Q. Li, M. Young, V. Naing, and J. Donelan, "Walking speed estimation using a shank-mounted inertial measurement unit," *Journal of biomechanics*, vol. 43, no. 8, pp. 1640–1643, 2010.

[33] S. Yang, C. Mohr, and Q. Li, "Ambulatory running speed estimation using an inertial sensor," *Gait & posture*, vol. 34, no. 4, pp. 462–466, 2011.

[34] M. Grimmer, M. Eslamy, and A. Seyfarth, "Energetic and peak power advantages of series elastic actuators in an actuated prosthetic leg for walking and running," in *Actuators*, MDPI, vol. 3, 2014, pp. 1–19.